"BABEȘ-BOLYAI" UNIVERSITY OF CLUJ-NAPOCA

FACULTY OF BIOLOGY AND GEOLOGY

Doctoral School of Theoretic and Applied Geology

GEOGENIC RADON IN RELATION TO INDOOR RADON CONCENTRATION.

CASE STUDY: CLUJ-NAPOCA

SUMMARY

Author:

ȘTEFAN FLORICĂ

Scientific adviser:

Prof. Univ. Dr. VLAD A. CODREA

Cluj-Napoca, 2022

Keywords

Contents

Introduction

Radioactivity has been of interest to the scientific community since Henri Becquerel discovered it in 1896. The study of radioactivity has led to the development of a field of its own, radiation protection, which studies the effects that ionising radiation has on the human body.

The harmful effects of ionising radiation on organisms are well known and have been highlighted by sadly remembered events in recent human history: the Chernobyl nuclear accident, the nuclear bombs dropped on the population at Hiroshima and Nagasaki, nuclear tests in various parts of the world, etc.

While man-made radioactivity can have a catastrophic and immediate impact on the environment, another, subtler enemy can have an equally harmful impact in the long term. Natural radioactivity is the main source of radiation to which the entire population of the globe is exposed, to varying degrees depending on the geo-topographic location and geological characteristics of the earth's crust. Alongside terrestrial radiation, generated by carbon, potassium and uranium isotopes - found in varying amounts in all types of rocks, soils and waters - cosmic radiation also plays an important role in the total irradiation of the population.

Radon is considered the main source of exposure to ionising radiation for the population and in recent years has been one of the most studied environmental carcinogens, being classified by international organisations specialised in radiation protection as a category I carcinogen. Although the harmful effects of radon and its progeny on the lungs are well known - demonstrated by numerous epidemiological studies that have shown a correlation between increased radon levels and lung cancer - its impact on the whole body is still unknown.

As an inert gas, radon has the ability to infiltrate and accumulate in enclosures in significant concentrations that can cause serious health problems. Recommendations from international organisations specialising in public health and radiation protection stipulate the need for systematic measurements and the establishment of reference levels of radon exposure, as well as the identification of risk areas characterised by a high radon potential.

The international recommendations have been transposed into European legislation by Council Directive 2013/59/EURATOM of 5 December 2013 laying down basic safety standards for protection against the dangers of exposure to ionising radiation. It thus becomes mandatory for all European states to develop national action plans to address the risks arising

from exposure to radon and to set reference levels of indoor radon concentrations not exceeding 300 Bq/m^3 (the international unit of measurement of radioactivity is the becquerel). While the EU directive only provides recommendations for private dwellings, it becomes mandatory for workplaces and places with public access. Member States must therefore ensure, through their own specific legislation, dose limits, measurement of radon levels and the implementation of remedial solutions - if the concentration exceeds the reference level set by each country.

The EURATOM Directive has also been transposed into Romanian legislation, where the reference level has been set at 300 Bq/m^3.

With the implementation of the European Directive, most of the Member States that have joined it have undertaken scientific studies on the establishment of radon risk zones. There have been a wide variety of approaches, but at present, the European radon risk map drawn up in accordance with the recommendations of the Joint Research Centre (JRC) has only involved residential measurements. The map is divided into 10 x 10 km (100 km^2) grid cells and the measured values for each cell are plotted as arithmetic means. Such an approach has some limitations and should therefore be viewed with some caution. Newer approaches also consider other variables such as soil permeability, soil pedology, soil radioactive metal content and geology.

It is well known that geology is the main source of the radioactive elements from which radon originates. Most approaches to mapping geogenic radon and radon potential are based on the geological component. What is the relationship of geogenic radon to indoor radon, what are the pathways and what variables influence the migration and accumulation of radon in enclosures, are questions that are country-specific.

This paper aims to answer some of these questions and to contribute, together with the existing studies in Romania, to a more in-depth knowledge of the radon problem.

Chapter 1: Radon

Radon is a radioactive gas that is ubiquitous in the environment. It is naturally generated and its presence is interdependent with the decay series of uranium - an element found in all types of rocks and soils, in greater or lesser quantities, depending on their genesis. Radon can migrate from rocks to soil and then seep and accumulate in building enclosures, at concentration levels that can be medically problematic. Research in recent years has shown

that it is the main source of radiation in the population and is classified as a category I carcinogen (IARC, 1988; ICRP, 2007; UNSCEAR, 2008; WHO, 2009).

Radon ($_{86}$Rn) has 37 known radioactive isotopes, from ^{195}Rn to ^{231}Rn. Due to their short half-lives, most of these isotopes do not make a significant contribution to natural exposure, as they are much more likely to decay before reaching the atmosphere than radon. On the other hand, the ^{222}Rn isotope, a descendant of ^{226}Ra and originating from the ^{238}U series, has a half-life of 3,8 days, which is long enough for it to accumulate to significant concentrations. Radon per se is not of particular consequence in the irradiation of the population, but rather the decaying progeny that actively contribute to internal and external irradiation. These are the radioactive isotopes ^{218}Po, ^{214}Pb, ^{214}Bi and ^{214}Po, which originate from the uranium series (^{238}U) and are also known as radon progeny (Figure 1).
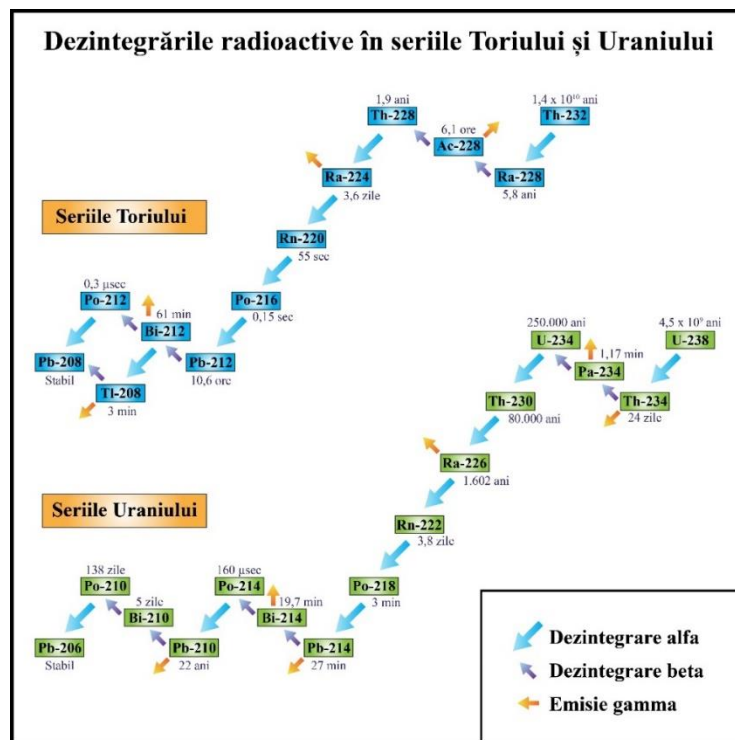
Figure 1. Uranium and thorium decay series and their progeny products (redrawn after Ud-Din Khan and Nakhabov, 2020).

Radon is continuously formed in the Earth's crust by the decay of uranium in various mineral associations. Characterised by high chemical activity, uranium readily reacts with other chemical elements, leading to the formation of both uranium minerals and uranium-bearing accessory minerals. Although the crustal abundance of uranium is relatively low (2,7 ppm), 5 % of currently known minerals contain uranium as a major constituent. In addition, accessory uranium-concentrating minerals are much more numerous.

In magmatic rocks, uranium occurs as uranium minerals, uranium-bearing minerals and as a substitutional element in the crystal lattices of some minerals. Uranium may also be adsorbed on the surface of crystals and grains or may be present in the intergranular space. Last but not least, it can be encapsulated in fluid inclusions of minerals or in structural defects in crystal lattices, including on cleavage planes. In magmatogenesis, uranium accumulates in the final phases of magmatic differentiation and has a particular affinity for acidic rocks. The quantitative geochemical distribution of uranium in magmatic rocks shows an increase in uranium concentrations from basic and ultrabasic to intermediate and acidic rocks (e.g., Stoici and Tătaru, 1988; Cosma and Jurcuţ, 1996; Murariu, 2005). A positive correlation is also observed between uranium content and SiO_2 and K_2O, and a negative correlation with CaO content (Stoici and Tătaru, 1988).

In Romania, the highest mean values of magmatites radioactivity were determined in rhyolites and granites, and the lowest values in dunites, gabbros and basalts (Stoici and Tătaru, 1988), thus confirming the trend of increasing concentrations of radioactive elements with magmatic differentiation.

The uranium content of metamorphic rocks depends mainly on the composition and nature of the parent rocks undergoing metamorphic processes and less on the degree of metamorphism or age of the metamorphites (Murariu, 2005). Through burial, under the influence of high temperatures and pressures, parent rocks metamorphose (and sometimes melt), which favours uranium fractionation and concentration (Klepper and Wyant, 1957).

Similar to magmatic rocks, in metamorphic rocks uranium is formed both in the parent minerals, but also frequently occurs in accessory minerals, e.g. zircon and apatite. More rarely it fills structural defects in the crystal lattice, is adsorbed on the surface of the mineral grain, or is attached to cleavage planes (Ahmad and Wilson, 1981).

From the research carried out in Romania on the quantitative distribution of radioactive metals in metamorphites, it appears that the metamorphic rocks with the highest uranium content are the Tulgheş Group epimetamorphites, at the opposite pole are amphibole rocks, quartzites, crystalline limestones and dolomites (Murariu, 2005). Microcline gneisses contain more uranium than plagioclase gneisses, and in the Someş Group (Apuseni Mountains), mica-schists contain more uranium than amphibolites (Stoici and Tătaru, 1988; Murariu, 2005).

In sedimentary processes, uranium accumulation in rocks depends on its migration capacity in natural waters and deposition from solutions under the action of reducing agents

and adsorbates. The mobility of uranium is mainly conditioned by water chemistry and pH and Eh values (Murariu, 2005; Cumberland et al., 2016). Organic matter, through enzymatic reduction, bio-sorption, bio-mineralization and bio-accumulation phenomena associated with bacteria, influences the oxidation state and consequently the mobility of uranium. The resulting biogenic uranium can thus easily undergo reoxidation and remobilization processes over time (Cumberland et al., 2016; Rallakis et al., 2019).

Sedimentary rocks can contain from a few ppm U to several tens of thousands of ppm U, as is the case of black sands (38750 ppm U) and black clays (19400 ppm U) in the Coutras region of France (Murariu, 2005). In Romania, sedimentary rocks have been insufficiently studied in this context. Stoici and Tătaru (1988) place most sedimentary rocks close to the mean of 3 ppm U. The highest concentrations of radioactive elements are found in clayey shales and clays, followed by sandstones, microconglomerates and conglomerates. The lowest concentrations are measured in carbonate rocks (Stoici and Tătaru, 1988).

1.1. Radon exposure

1.1.1. *Health effects*

According to the report by the United Nations Scientific Committee on the Effects of Atomic Radiation (UNSCEAR, 2008), radon inhalation (1,26 mSv) is the primary source of ionizing radiation exposure for the population, accounting for 42 percent of the mean exposure. Numerous epidemiological studies on animals and humans have proved the harmful effects of radon and its progeny, which emit alpha particles. International organizations for public health and radiation protection have classified radon as a category I carcinogen (IARC, 1988; ICRP, 2007; WHO, 2009). Even though radon contributes to whole-body irradiation, the lung is the target organ. Numerous studies have demonstrated that radon exposure directly causes lung cancer (Cross, 1998; Darby et al., 2005, 2006). Smoking continues to be the greatest cause of lung and respiratory tract cancer, while radon is the leading cause of lung cancer in nonsmokers (WHO, 2009). If a smoker is exposed to an environment with high radon concentrations, his or her cancer risk is significantly increased. Due to the size of their lungs, children are also at a significant risk for radon exposure since their breathing rate is faster, resulting in a higher rate of radon inhalation (Keith et al., 2012).

The pathophysiological effects of radon are primarily related to its decay products which emit alpha, beta, gamma and X-rays. Alpha radiation has a much stronger radiobiological effect than beta or gamma radiation, as the changes it produces in DNA can

lead to chromosomal aberrations or even breakage, which can give rise to carcinogenic processes. Although radon can be easily exhaled, its decay products such as ^{218}Po, ^{214}Po, ^{214}Pb, ^{214}Bi can attach to aerosol particles and form clusters that can attach to suspended particles. The latter will be inhaled and deposited throughout the respiratory tract and especially in the lung, where radioactive alpha decay will cause DNA damage, ultimately leading to the onset of cancer (Cosma et al., 2009; Keith et al., 2012).

1.2. Legislative regulations

Individual data from 13 European countries (Darby et al., 2005) supported the idea that the generation of lung cancer pathology is proportional to increased radon exposure. In this context, the Council of the European Union adopted Directive 2013/59/EURATOM where it stipulates the requirement for each Member State to establish a national action plan for the reduction of lung cancer attributable to radon exposure of the population, both in dwellings and workplaces and buildings with public access.

The Directive has also been transposed into Romanian legislation, where the reference level for the annual mean concentration of radon activity in indoor air (workplaces, homes, buildings with public access) is set at 300 Bq/m^3 (M.O. 752/3.978/136/2018). It should be remembered that the reference level is not a limit, but rather the concentration over which prolonged exposure to radon should be avoided. Radon concentrations must be measured, monitored, and remedied in all public buildings and workplaces, and it is recommended that the same be done for residential dwellings.

In 2019 the Order of the President of CNCAN (National Commission for the Control of Nuclear Activities) no. 185/22.07.2019 was issued regulating the Methodology for the determination of radon concentration in indoor air.

Chapter 2: Radon measurement methods and equipment

2.1. Methods and equipment used in the thesis to measure radon in air

In the indoor radon measurement campaigns, the passive approach using CR-39 trace detectors was utilized, along with the RadoSys 2000 assembly (Elektronika, Budapest, Hungary) consisting of an etching bath and an optical microscope with automatic readout.

2.1.1. *The passive method – tracking detection technique*

Radon measurement using tracking detectors is the most viable and common technique for measuring radon in air in Europe (Cinelli et al., 2019). The polymer from which the CR-39 tracking detector is made, namely alidiglycol, is sensitive to radiation in the 0,2-20 MeV range, which leads to molecular chain breakage and the appearance of the crossing tracks. In order for these traces to be read and interpreted to calculate the (mean) radon content, CR-39 detectors are chemically etched.

The etching process starts with the preparation of the detectors, which are placed on a plastic slide. As hazardous chemicals are handled, all steps are carried out in chemical niches with exhaustion. Solution preparation takes place in an RB4 Etching Unit. Four litres of distilled water are heated to 90 ˚C, after which 1 kg of sodium hydroxide (NaOH, 99.98 % concentration, Merk KgaA, Germany) is gradually added. The detector slides are then inserted into a carousel along slits and then introduced into the prepared solution, taking care that the temperature of the solution does not exceed 92 ˚C. The slides are automatically rotated in the solution at a constant temperature of 90 ± 2 ˚C for 4 hours and 30 minutes. This process is called chemical engraving and is intended to enlarge the traces on the detectors to microscopically observable sizes. After the etching process is complete, the hydroxide solution is drained into special storage containers and the neutralization process begins. Five litres of 1 % HCl solution is added, in which the detectors are washed for 20 minutes. At the end of the 20 minutes the HCl solution is collected in a container for reuse and replaced by 5 litres of distilled water in which the slides are rinsed for a further 20 minutes. After completion of the neutralisation process, the slide carousel on which the detectors are placed will be removed from the etching bath and allowed to dry for several hours at room temperature. Once the slides are dry, the detectors are wiped with isopropyl alcohol and placed in the automatic reading optical microscope. The Radometer 2000 microscope produced by RadoSys Ltd. (Hungary) is a self-focusing scanning microscope that has the ability to count the number of traces produced by alpha radiation, i.e. the density of traces on a 50 mm^2 area.

The mean radon concentration is calculated from the track density using the formula (Dinu, 2009; Cucoș (Dinu) et al., 2012):

$$C_{Rn} = \frac{\rho \times Fc}{t}$$

Where: C_{Rn} – calculated radon concentration (Bq/m^3), ρ – measured track density (tracks/mm^2), Fc – calibration factor (kBq/h/m^3)/(tracks/mm^2), t – exposure time (h).

In order to reduce measurement errors and to verify the accuracy of the RadoSys 2000 system, the LiRaCC laboratory regularly participated in international intercomparison exercises with internationally validated laboratories.

2.1.2. *Intercomparison of passive method results*

Over the last 7 years, the passive measurement method, with CR-39 track detectors, has been tested and validated by participating in 6 international intercomparison exercises. Four of these were carried out by the BfS laboratory (Bundesamt fur Strahlenschutz, Germany), which is accredited by the German accreditation body (Deutsche Akkreditierungsstelle) for the calibration of devices measuring the activity concentration of radon and its decay products in air. Full details of the procedure and the results obtained from participation in the intercomparison organised by the BfS have been published in intercomparison reports by Foerster et al. (2016, 2019), Friedrich et al. (2019) as well as in review reports.

For the years 2015, 2019 and 2020 there was no deviation from the proposed limits, and the accuracy of the measurements is more than satisfactory. For the intercomparison in 2018, the data showed 3 deviations, two of which are significant, being recorded for group 1 (203 kBqh/m^3) and group 4 (1676 kBqh/m^3). One of these deviations is just below the lower limit and was recorded in group 2 (221 kBqh/m^3). In all cases, the measured value was underestimated compared to the reference value. With the exception of group 1 in the 2015 intercomparison, which had a relative error of 11,3 %, and group 1 in the 2019 intercomparison, where the relative error was calculated to be 10,4 % - but with no deviations within them - all other detector groups in all years had relative errors well below 10 %, including groups 1, 2 and 4 where deviations were reported.

Given that the equipment used in the study has been calibrated regularly by the manufacturer, in compliance with international quality standards, and that international intercomparison exercises show that there are no systematic deviations from one year to the next, we can assume that the deviations recorded in the 2018 intercomparison are not due to measurement errors but rather to random errors related to the influence of the etching process on the detectors, given by differences in the thickness of their layers (Leung et al, 2007) or result from differences in the geometry of the film exposure inside the detector housing as well as the variability of the diffusivity property of the detectors (Zhukovsky et al., 2010). Taking

all these aspects into account, we can conclude that the working methodology of the LiRaCC laboratory meets the international standards for passive trace detector measurements and the measurements performed throughout the study can be considered to have a high accuracy.

2.2. Methods and techniques used in the thesis for radon measurements in soil

Measurement of radon activity in air originating from soil is usually performed by detecting radioactive decays in a soil gas sample. The most commonly used method for this purpose is the active method (Cinelli et al., 2019). For this study we used the active method with two different measurement techniques: scintillation detectors and ionization chambers. Details of the apparatus and protocol used in the detection of radon in soil-derived gas are described below.

2.2.1. *Scintillation chamber technique*

The LUK3P measuring instrument (Jiry Plch, Czech Republic; see Plch, 2008) measures radon in air samples, using the Lucas cell scintillation technique. The main part of the instrument is a photomultiplier tube that allows the insertion of a cylindrical capsule lined with scintillator material (zinc sulphate), which together form the detection chamber. The volume of the Lucas cell is 145 ml and the total volume of the detection chamber is 150 ml. The detection chamber is fitted with a lid that allows it to be hermetically sealed. The sample is introduced into the detection chamber using a syringe (Janet, 150 ml) by creating a negative pressure using a manual vacuum pump. The pressure in the detection chamber can be modified by means of a tap, and its levels are monitored with an electronic barometer connected to a microprocessor, which in turn controls the filling process of the chamber. The light pulses generated by the alpha particles on impact with the scintillator layer are captured by the photomultiplier, amplified and passed through an amplitude differentiator (which differentiates them from the background noise) and then converted into electrical pulses which are counted and converted into radon concentration, also by the microprocessor. The microprocessor is linked to a memory, a display and control elements that turn it into a real mini-computer.

The electronic components are powered by a rechargeable 2,5 Ah Li-Ion battery and the connection with other computers, where data can be downloaded from the internal memory of the device, is via an RS232 port. The internal memory of the instrument allows the storage

of 12573 measurement results, statistically processed (e.g. calculation of mean and standard deviation of the results) using a pre-installed program (Plch, 2008). Each measurement uses a separate Lucas cell, which will be left to decontaminate for a minimum of 3 hours before being reused.

2.2.2. *Ionising cells technique*

The RM-2 system for radon measurements in soil has been specially designed for soil measurements by the Radon v.o.s. company from the Czech Republic. The detection principle is the ionisation chamber operated by an electric current. The system consists of a set of ionisation cells (IK-250) with a volume of 250 ml and an ERM-3 electrometer (voltage reader).

The detector operates in the unsaturated mode of a volt-ampere characteristic, the voltage between the electrodes and the ionisation chamber being 48V. The detector's electric current sensitivity at this voltage is 85 % of the saturated current. The direct ionization current is amplified and then electronically and statistically processed. The result is shown on the display of the device and automatically recorded in its memory. The actual measurement time is 120 s which is divided into two types of processing. The first 80 s are necessary for the stabilisation of the system, during the next 40 s the radon concentration is calculated based on the statistical analysis of the values resulting from the current measurements (according to the RM-2 technical manual).

2.2.3. *Intercomparison of results obtained by the active method*

In order to test the effectiveness and accuracy of the equipment used in this study, and not lastly to maintain quality standards with regards to radon measurements in different environmental factors, a metrological test of active and passive equipment and two international intercomparison exercises of radon measurements in soil were performed. The metrological test of the LUK3P radon detector indicated a good measurement accuracy of the device.

2.2.3.1.   *Intercomparison exercises of radon measurements in soil*

In September 2018 and September 2021, respectively, we participated in the international comparative measurement of radon in soil at the radon reference sites Cetyne and

Buk in the Czech Republic, administered by the Faculty of Science of Charles University in Prague. The aim of these exercises was to check both the accuracy of the instruments for calibration and the procedure for radon measurements in the field. For both campaigns the same measurement design system was maintained and the same measurement protocol was applied using the same equipment.

The comparative measurement for the year 2018 shows that the radon data are overestimated (RIM, 2018), and the one for the year 2021 shows that the radon data meets the test criterion, the measurement accuracy being in line with international standards (RIM, 2021).

2.3. Methods for assessing radon potential in soil

The radon potential of a site is based on the relationship between radon concentration and soil permeability. Thus, soil permeability becomes the second most important parameter, after concentration, for determining radon potential.

Permeability can be determined by direct, in situ measurements or by assessing the grain size of a soil sample. The disadvantage of the latter method is that it does not consider other variables such as soil moisture and density or effective porosity. Thus, the actual permeability of the soil during radon concentration determination can only be determined by *in situ* measurements.

In the present project two ways of permeability determination were used, one with the Radon-Jok permeameter (Radon v.o.s. from the Czech Republic) and the second with the Bottle-device designed and developed by the LiRaCC laboratory researchers (Papp, 2011). Both methods have been tested and calibrated.

2.3.1. *Neznal radon potential method*

Neznal et al. (2004) proposed a soil radon risk assessment model based on radon concentration and soil permeability measurements. Depending on the radon potential, three categories of risk or radon index (RI) can be identified. As can be seen in the diagram in Figure 2, the risk categories are delimited by a dotted line and divided into low, medium and high.
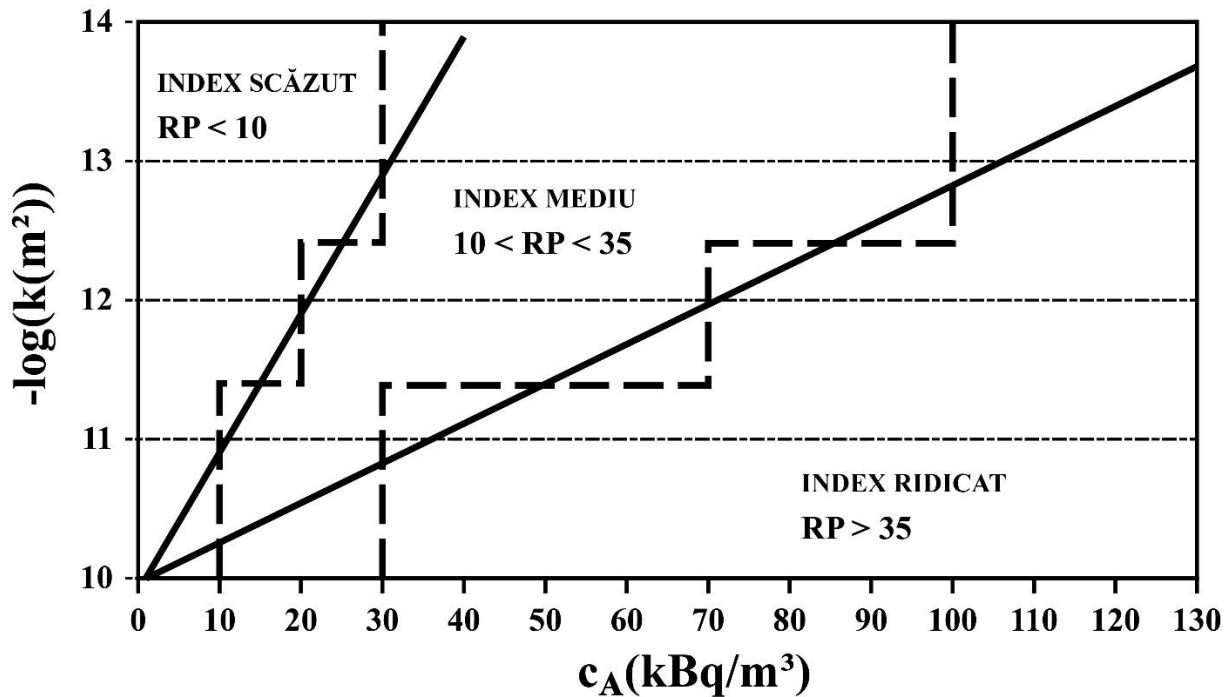
Figure 2. Neznal Radon Potential and Index (Neznal et al., 2004, redrawn).

Therefore, based on the calculated radon potential values, the risk index of the site is set as low (RP <10), medium (10 ≤ RP <35) or high (RP ≥ 35) (Neznal et al., 2004).

2.3.2. *Kemski radon potential method*

Kemski et al. (2004) developed a method for assessing geogenic radon potential and proposed a distribution grid of values divided into 7 potential classes (0 to 6) according to the relationship between concentration and permeability. Based on this method, a radon potential map of Germany was subsequently produced.

For radon concentration in soil 5 categories of concentration levels are used: a) values below 10 kBq/m^3, b) values between 10 and 30 kBq/m^3, c) values between 30 and 100 kBq/m^3, d) values between 100 and 500 kBq/m^3 and e) values above 500 kBq/m^3. Permeability is also divided into a) low, b) medium and c) high. Depending on the ratio between radon concentration and permeability, the radon potential class will result, where 1 means the lowest potential and 6 the highest (Figure 3).
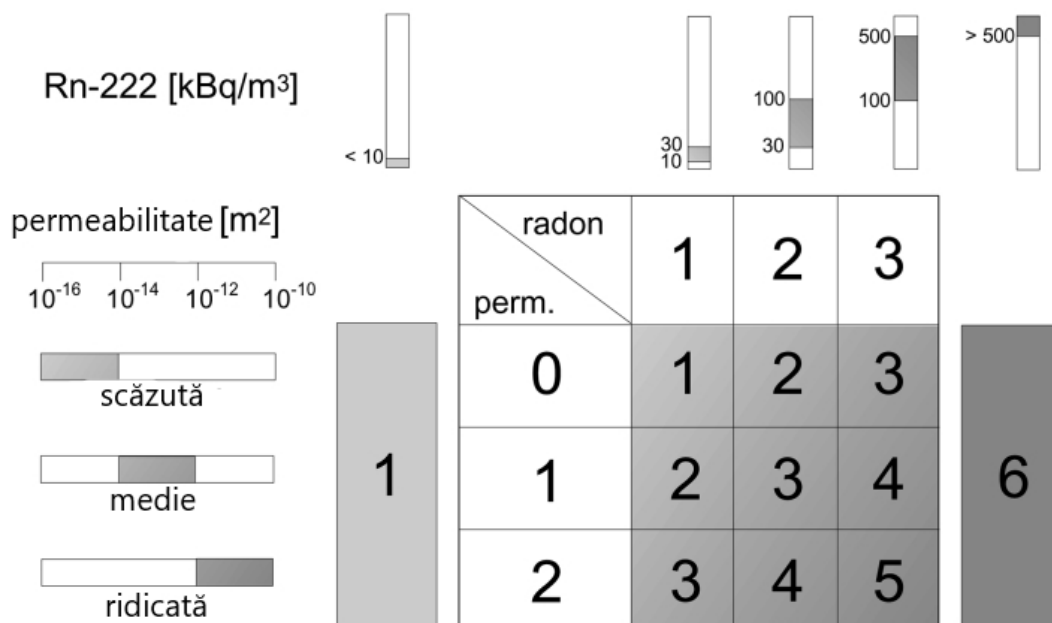
Figure 3. Radon potential categories according to Kemski et al. (2004).

2.3.3. *Radon diagnosis of buildings*

The diagnosis included a set of measurements, standardized according to ISO 11665-8:2019, to identify radon sources and pathways into the building, the main aspects are described below.

The radiometric measurement involved quantification of surrounding gamma radiation as well as from ground contact and building materials. This allows the identification of areas showing higher doses, characteristic of the presence of ^{226}Ra and its decay products. Gamma dose rate measurements were carried out with the Gamma Scout. Furthermore, soil and building material samples were collected and investigated by high-resolution gamma spectrometry to measure ^{226}Ra activity. The method is extensively described in the paper by Cosma et al. (2013).

The "spot" measurement protocol described in Neznal et al. (2004) was used to identify the presence of radon in the air in cracks and ducts. Air samples were collected using a syringe (Janet, 150 ml) with a needle directly from visible cracks or ducts before they emerged and diluted into the indoor air, and then measured for radon activity concentration determination with RTM-2 (Sarad GmbH, Germany) and Luk 3P (Jr Plch, Czech Republic) devices. The working method is similar to that of soil measurements.

The estimation of the radon exhalation rate from the floor surface involved measuring the radon activity concentration by accumulating radon in an enclosure of known volume and area. Rad7 (Durridge Company Inc., USA), Alpha Guard (Saphymo GmbH, Germany) and RTM1688-2 (Sarad GmbH, Germany) were used to make these measurements, the method being extensively described in Neznal et al. (2004).

For all 100 sites, the radon potential of the soil around the building was determined using the Neznal et al. (2004) method.

Other data, on parameters such as humidity, pressure, temperature but also concentration of volatile organic substances, CO_2 and CO were collected using the ICA system, developed by the LiRaCC laboratory for the SMART-RAD-EN project (Tunyagi et al., 2020). Also, using specially designed questionnaires, data was collected on the architectural and construction details of the buildings, such as the type of floor and joinery of doors and windows, the existence of concrete screed, the type of heating system, etc.

Chapter 3: Research stages

The research was carried out in several stages, each of which generated its own results, which are integral parts of this thesis. In this chapter I will present all the stages of the research, up to the Cluj-Napoca case study, which I will describe and analyse in later chapters.

3.1. National radon distribution in soil and water

The first phase of the present study was initiated within the RAMARO project (PN-II-PT-PCCA-2011-3.2-1064 - Radon map (residential, geogenic, water) for the Central, Western and North-Western regions of Romania) - in which data were collected to produce the first radon map of water and soil in Romania. The aim of this approach was to identify radon priority areas based on soil and water measurements. Data from the SMART-RAD-EN project were also partially included in this study. The study was published in Burghele et al. (2019), and the most important results of this analysis will be presented below.

The investigated area represented approximately 42 % of the Romanian territory and covers Transylvania, Maramureș, Crișana and Banat, totalling 16 counties with a total of 99,837 km^2. Soil measurements were carried out following the Neznal el al. (2004) protocol with the Luk3C equipment (an older version of the Luk3P equipment already presented in chapter 2, with the same technical specifications and measurement protocols). Water samples

were also measured with the Luk3C equipment, using the Luk-VR system following the method presented in Cosma et al. (2008). The measurement protocol aimed at dividing the territory into 10×10 km² cells, following the JRC (European Commission - Joint Research Centre) recommendations presented in Tollefsen et al. (2014). The minimum number of measurements per cell was 1 and the maximum 17, with a median of 3, which was valid for both soil and water samples, although the latter were collected according to availability, from different wells, springs and other drinking water sources. Summary statistics of radon measurements in soil and water samples are presented in Table 1.

Table 1. Summary statistics for radon measurements in soil and water.

Measurment type	Nr.	Min.	Max.	A.M.	S.D.	G.M.	G.S.D.
Rn in soil (kBq/m³)	2564	0,2	179	29,3	17,4	24,5	1,9
Rn in water (Bq/l)	2452	0,3	352	9,8	16,9	6,2	2,7

AM – arithmetic mean; SD – standard deviation; GM – geometric mean; GSD – standard geometric deviation.

Geologically, the study region consists of a mixture of magmatic, metamorphic, and sedimentary deposits of varied ages that constitute key structural assemblage components (Figure 4). The most important structural assemblage is represented by the folded regions that create the Carpathian branches that border the Pannonian and Transylvanian Depressions, circumscribing the latter (Săndulescu, 1984; Mutihac, 1990). The representative Carpathian units for the area under study are partially represented by the Eastern and Southern Carpathians, while the Apuseni Mountains are fully represented. Additionally, the internal depressions and neighboring areas were completely covered.

The data were analyzed statistically using GraphPad Prism 5.0 software, and their statistical distribution was examined using the Shapiro-Wilk test. In addition to the Kruskal-Wallis non-parametric test, Dunn's post-hoc analysis was performed to compare the medians of the measured samples. Log-transformed data were used to calculate the Pearson correlation coefficient to estimate the relation between the measured variables (Table 2). The alpha significance level was set at 0.05, and maps of radon distribution in soil and water were generated using the ArcGIS 9 program (Figures 5 and 6).
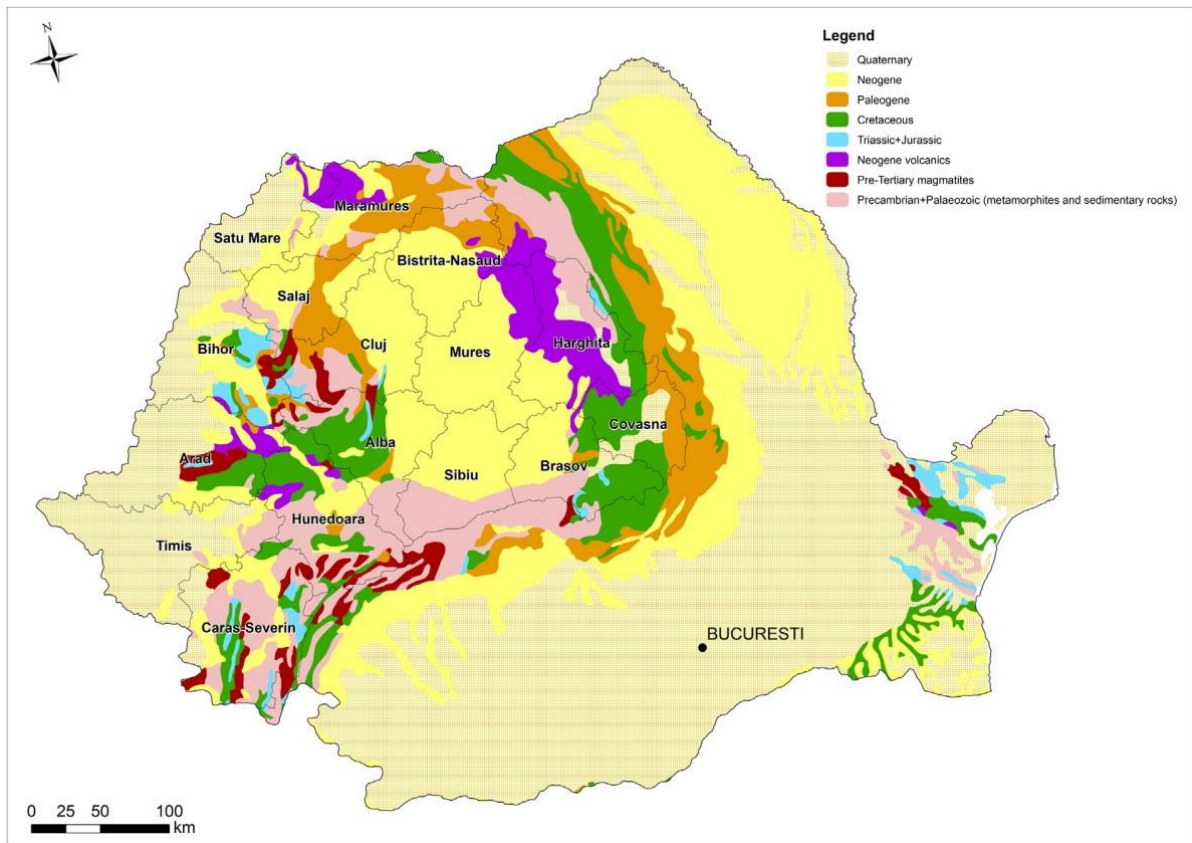
Figure 4. Simplified geological map of the studied countys (after Săndulescu et al., 1978; from Burghele et al., 2019).

Table 2. Pearson correlation coefficient of log-transformed data of radon measurements in soil and water (from Burghele et al., 2019).

Type of analysis	All data	All cells	≥ 2 measurments/cell	≥ 2 measurments/cell	≥ 2 measurments/cell	≥ 2 measurments/cell
$r_{sd-water}$	0,16	0,36	0,33	0,28	0,47	0,46
Data number	1702	648	495	351	85	45
p	<0,01	<0,01	<0,01	<0,01	<0,01	<0,01
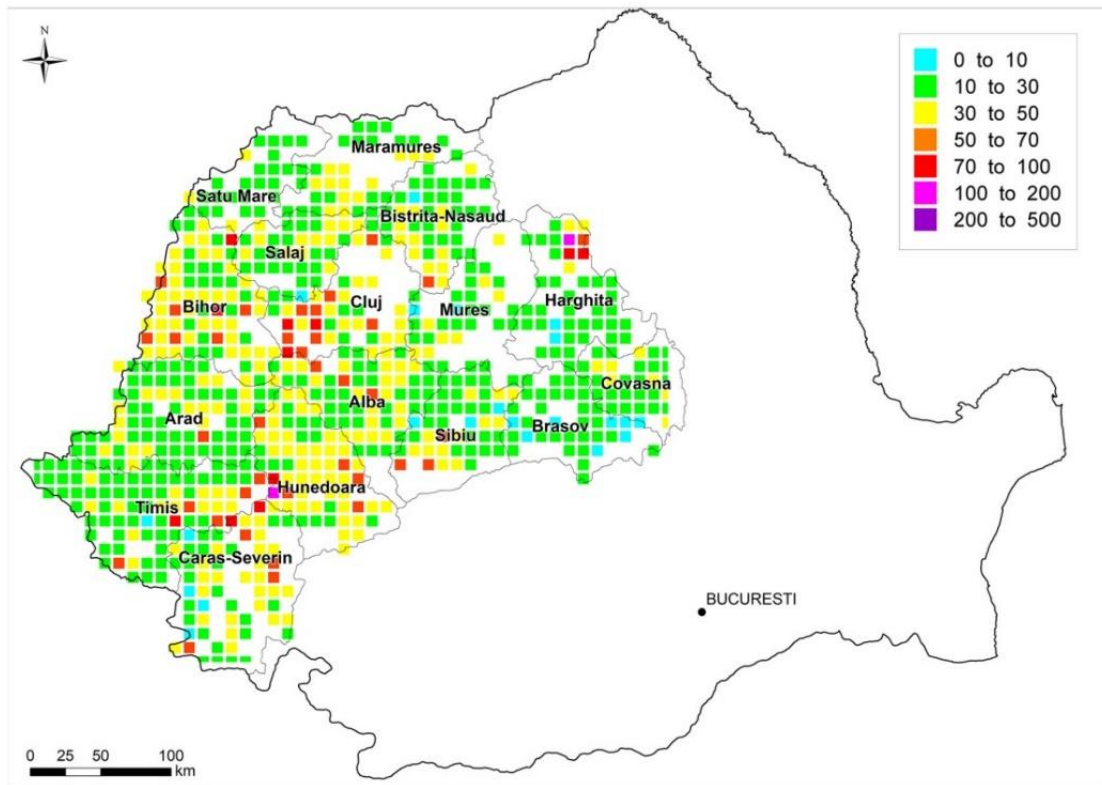
Figure 5. Arithmetic mean of radon concentration values in soil air samples for 10×10 km (from Burghele et al.,
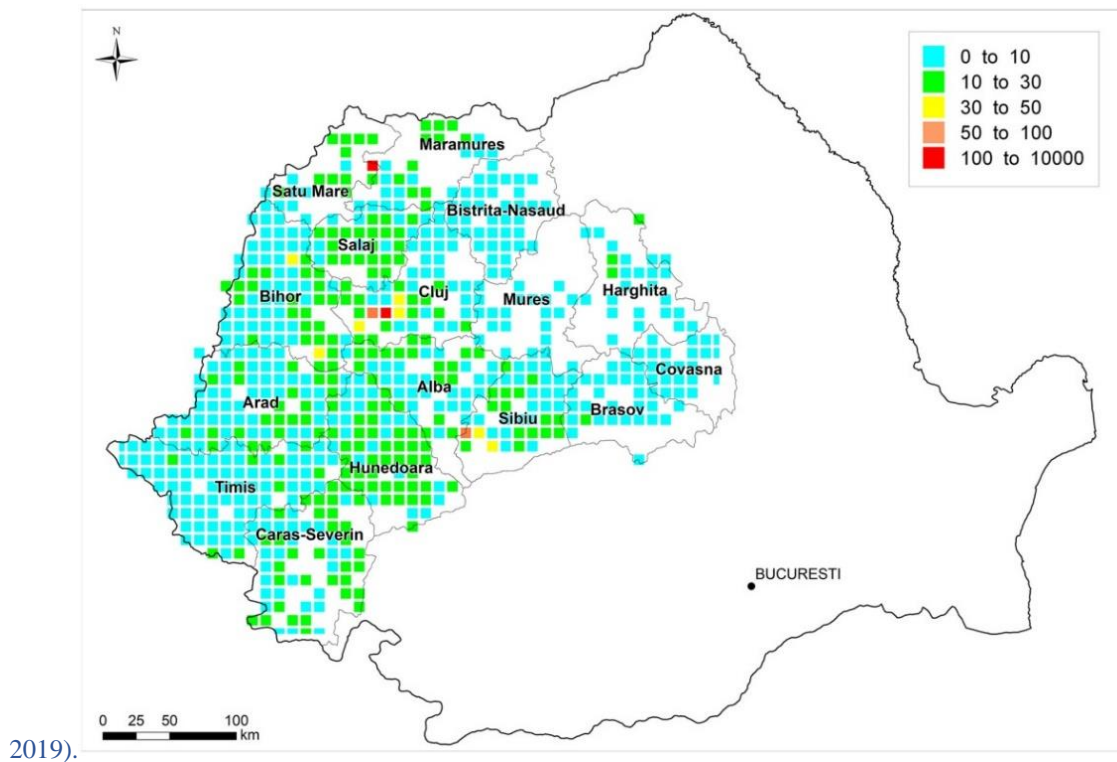
2019).

Figure 6. Arithmetic mean of radon concentration values in water samples for 10×10 km (from Burghele et al.,

2019).

After division into polygons of 10×10 km^2, it was observed that 12 % of the resulting 1111 cells correspond to mountainous areas with a sporadic population, which is why they were not taken into the study. Therefore, the 2564 soil measurements and 2452 water measurements were merged into 761 and 649 cells respectively. The arithmetic mean radon concentration measured in soil was 29,3 kBq/m^3, with limits ranging from 0,2 to 179 kBq/m^3, these values being comparable to those reported for European soils (Beaubien et al., 2003; Al-Khateeb et al., 2017). The geometric mean was 24,5 kBq/m^3 and corresponds to values previously reported in Romania by Cucoș et al. (2017) and Papp et al. (2017). By applying the Shapiro-Wilk test, the normal distribution of the log-transformed data was not confirmed, which may be due to atmospheric parameters that may influence radon activity in soil. Instead, a good negative correlation between radon concentration in soil and atmospheric pressure was obtained. By applying the non-parametric Kuskral-Wallis test and Dunn's post-hoc analysis, a statistically significant difference was obtained between the median values of soil measurements taken in August and the rest of the months, as well as June vs. January and June vs. October. A statistically significant difference was also observed between the warm and cold seasons, with radon activity in soil being significantly lower in the summer months compared to the winter months. This may be due to low soil moisture in summer, which will lead to reduced radon diffusivity.

By examining geological patterns, it is evident that the Transylvanian and much of the Pannonian Depression have relatively low soil radon concentrations, while Bihor County's Western Plain has moderate levels. The high values are characteristic of the metamorphic regions of the Carpathian Units, particularly in the Central-Carpathian region and the edge of the Pannonian region, as well as in the Western Carpathians, and thus explain the chemical composition of the rocks that make up these regions.

The majority of the water samples were gathered from wells (69 %), followed by tap water (27 %), and only 4 % from spring water. The arithmetic mean of radon concentration activity in all water samples was 9.8 Bq/l, which is 10 times lower than the recommended limit value of 100 Bq/l [EU, 2001; WHO, 2011; Law nr. 301/2015 establishing the requirements for the protection of human health with respect to radioactive substances in drinking water (published: 2015-12-07)]. Low concentrations of radon activity in water, up to 10 Bq/l, are typical in locations with largely sedimentary detrital deposits of Neogene age, such as the Transylvanian Basin and the western edge of the Apuseni Mountains. In addition, extremely low values were recorded for the Banat Plain. Mean radon values of 10-30 Bq/l were observed

in the southern Carpathians' western and central regions. High levels were measured in Quaternary sediments of the Western Plain, which can be linked to the western portion of the Apuseni Mountains, the source area for these deposits. Moreover, the mesometamorphic and granitic regions of the Apuseni Mountains had the greatest radon concentrations in water, with values averaging between 30 and 100 Bq/l and frequently exceeding 100 Bq/l.

The Pearson correlation coefficient calculated for soil and water sampling points close to each other showed a weak correlation (r = 0.16), but after all data were centralized at the cell level and 648 cells with at least one common collection point for soil air and water samples were identified, it suggested a moderate correlation between these two types of measurements (r = 0,36). As can be seen in Table 2, the correlation coefficient shows an increase in the degree of association between the two variables as the number of measured values per cell increases, but it remains moderate even when exceeding 6 measurements per cell (r = 0,47).

In conclusion, as far as drinking water in Romania is concerned, at least at the level of the present study, it does not present a significant contribution to indoor radon concentration, or a significant problem from a radiobiological point of view. However, as far as soil measurements are concerned, they may be an explanation for the radon measured indoors, particularly from a geological point of view, even if it has been shown later, in the studies presented below, that the variation of indoor radon concentration is also dependent on other factors.

3.2. The contribution of geogenic radon to indoor radon concentration

After the etching and reading of the first set of detectors (campaign from January to July 2017), the collected data for Cluj-Napoca were analyzed and evaluated to identify the next research stages. The main pertinent features of these results, which have been reported by Florică et al. (2017), will be presented below. Regarding the distribution of the data for Cluj-Napoca, the log-normal distribution was validated by the D'Agostino-Pearson statistical test (p > 0,05) after the first radon measuring campaign in chosen residences. 43 dwellings out of a total of 256 tested exhibited radon concentration values greater than 300 Bq/m^2. After using a seasonal correction factor to calculate an annual mean, the number of dwellings with radon levels exceeding 300 Bq/m^3 rose to 52. Thus, after the first measurement campaign, it was determined that 17 percent of the analyzed dwellings in the metropolitan area of the municipality of Cluj-Napoca had values in excess of the European reference level of 300 Bq/m^3 (Directive 2013/59/EURATOM). In addition, 20 % of the studied dwellings had radiation

levels above 250 Bq/m^2. The smallest concentration observed was 21 Bq/m^3, whereas the greatest value was 720 Bq/m^3. The geometric mean was calculated to be 95 Bq/m^3 while the arithmetic mean was 139 Bq/m^3 for all 256 dwellings. Consequently, the mean radon concentration recorded during this first campaign was greater than the European mean of 98 Bq/m^3 and equivalent to the values of 140-160 Bq/m^3 measured in the Czech Republic and Estonia. Using these data, a preliminary map of Cluj-Napoca was generated, in which the measurement results were compiled into 1x1 km cells using the same methodology as the European Radon Atlas (Cinelli et al., 2019). The range of measurements per cell is between 1 and 13, with a mean of 2 per cell. Thus, the total number of cells examined was 85, and eight percent of cells had arithmetic means more than 300 Bq/m^3 (Figure 7).
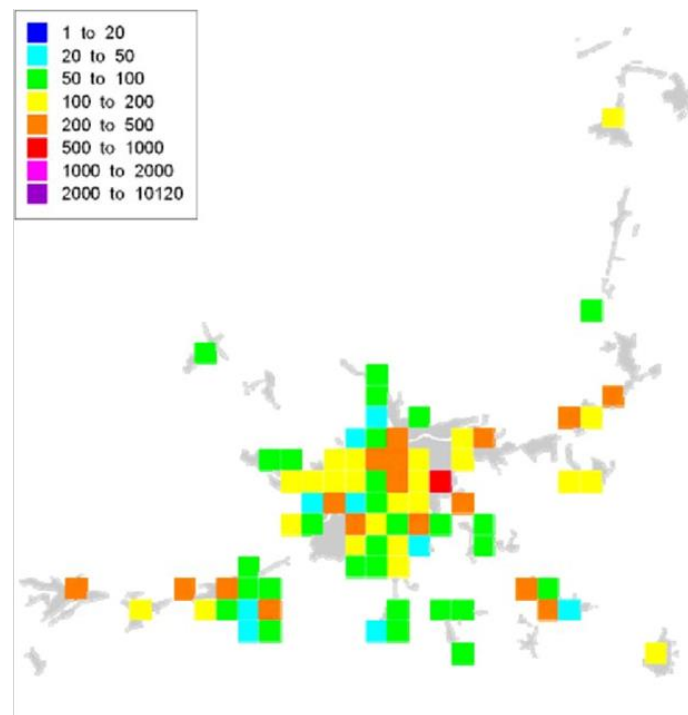
Figure 7. Indoor radon map for Cluj-Napoca municipality after the first measurement campaign of the SMART-RAD-EN project (from Florică et al., 2017).

This first campaign projected a fairly clear view of indoor radon concentrations at the level of the metropolitan area of the municipality of Cluj-Napoca, while indicating that geology may be the determining controlling factor in relation to their source, as a trend of high value distribution was observed for quaternary deposits. Further investigations were carried out to confirm these results.

3.3. Radon pathways into the interior

Following the screening with passive detectors (the two campaigns of 6 months each), diagnosis measurements were performed for 100 dwellings (from all 5 urban settlements: Iași, Bucharest, Timișoara, Sibiu and Cluj-Napoca) whose radon concentration values exceeded 250 Bq/m^3. The aim was to identify the pathways by which radon enters the indoor environment and, last but not least, which variables play a greater role in the accumulation and variation of indoor radon. The results of this research were published in Florică et al. (2020), and significant details will be reported below.

3.3.1. *Interpreting the results*

SPSS software, version 24, was utilized for statistical analysis of the data (SPSS Inc., USA). The D'Agostino-Pearson test was used to examine data distribution, and the nonparametric Mann-Withney test was used to compare variables. The 2 test (Chi-square) was used to determine the degree of association between the qualitative variables, and the Pearson correlation coefficient was calculated to determine the association relationships between the investigated parameters. As the dependent variable for multivariate analysis, log-transformed dwelling radon concentration data were utilized. In a stepwise regression approach, only factors with a statistically significant impact on the dependent variable are examined. The level of statistical significance was set at 0,05. Table 3 displays descriptive data for all monitored metrics in the 100 dwellings.

Table 3. Descriptive statistics of the parameters investigated in the 100 dwellings (from Florică et al., 2020, with changes).

Parameters	Min.	Max.	Median	A.M.	S.D.	G.M.
Residential Rn conc. (Bq/m^3)	150	1221	309	356	176	325
Φ max $(Bq/m^2/h)$	3	99	8	13	16	9
Q3 Rn_soil (kBq/m^3)	6	97	34	39	20	34
RP	5	133	29	33	21	28
CO_2 (ppm)	432	3375	1083	1213	638	1078
RH (%)	16	70	42	42	10	41
T (Cº)	13	31	21	22	3	22
Energy comp. (kWh/m2)	102	500	210	216	63	208
^{226}Ra (Bq/kg)	8	283	32	48	57	33

Φ_{max} este maximum value measured in exhalation; $Q3_{Rn}$ is the third quartile of measured radon concentration; RP is the radon potential; RH represents humidity; T is the temperature in Celsius degrees.

The normal distribution of the log-transformed residential radon concentration data was confirmed by applying the D'Agostino-Pearson test (p > 0,05). The arithmetic mean and geometric mean of the residential radon concentrations are 356 Bq/m^3 and 325 Bq/m^3,

respectively. These high values can be explained by the fact that the selection of the 100 dwellings in the present study had as main criterion a radon concentration above the threshold of 250 Bq/m^3.

For 33 dwellings the exhalation rate was below the detection limit, while in the remaining dwellings the exhalation rate showed high variations, with limits ranging from 10 $Bq/m^2/h$ to 358 $Bq/m^2/h$ and an arithmetic mean of 47 $Bq/m^2/h$. In 4 of the 6 dwellings where the exhalation rate was above 100 $Bq/m^2/h$, the floor is placed directly on the ground or slag, without concrete screed.

Cracks were identified in 88 dwellings, with an arithmetic mean of 6 cracks per dwelling. The maximum radon value measured at the cracks is 27 kBq/m^3 and the minimum value is 1 kBq/m^3, with a coefficient of variation of 85 %.

As for soil measurements, only in one dwelling they could not be carried out due to the presence of water in the soil at a depth of about 50 cm. For the calculation of the radon potential, the 75 % percentile (Q3) of the radon concentration in the soil was considered and the calculated value for Q3 ranged from 6 kBq/m3 to 97 kBq/m^3, with an arithmetic mean of 39 kBq/m^3. Radon potential (RP) values ranged from 5 to 133, with an arithmetic mean of 33. Thus, out of a total of 100 dwellings, 4 had a low radon index, 62 had a medium radon index and 33 had a high radon index.

Other indoor air quality indicators monitored in this study were CO_2 and CO. For the CO_2 concentration, values ranging from 432 ppm to 3375 ppm were measured with a geometric mean of 1078 ppm. In contrast, carbon monoxide was identified by measurements in only 10 dwellings, most likely due to the type of heating used during the cold season. Limits ranged from 0,1 ppm to 6 ppm and the mean concentration was 1,1 ppm.

Table 4 provides a summary of the statistical correlations between the parameters included in the bivariate analysis.

By calculating the Pearson correlation coefficient, an acceptable correlation was obtained between residential radon concentration and CO_2 concentration (r = 0,26, n = 97, p = 0,01), which indicates poor ventilation leading to accumulation of CO_2 as well as radon. No statistically significant correlation was observed between residential radon concentration and parameters such as exhalation, crack radon concentration, soil radon concentration, radon index and radon potential. The χ^2 test also confirmed that there was no statistically significant

dependence between residential radon concentration and radon index ($p > 0,05$). This means that the radon index cannot provide sufficient clues about residential radon levels and cannot be used as a surrogate for indoor radon measurements. An acceptable correlation was obtained between residential radon concentration and humidity ($r = 0,3$, $n = 97$, $p < 0,01$) and an inverse correlation between temperature and humidity ($r = -0,5$, $n = 97$, $p < 0,01$). An acceptable correlation was also obtained between CO2 concentration and energy consumption ($r = 0,3$, $n = 92$, $p < 0,01$). A good correlation was obtained between radon potential and ^{226}Ra content of soil samples ($r = 0,72$, $n = 10$, $p < 0,05$).

Table 4. Statistical correlations determined for the relevant parameters; where the correlation is significant at a level of 0.05* and 0.01** (from Florică et al., 2020, with changes).

Spearman correlation for ^{226}Ra	Soil	0,35	-0,07	0,5	0,65**	n/a	n/a	n/a	n/a
	Building material	0,008	0,55**	-0,17	-0,3	n/a	n/a	n/a	n/a
Variable		Indoor Rn	Φ max	Q3 Rn soil	RP	CO$_2$	Temp.	RH	Energy
Pearson correlation	Indoor Rn		0,05	-0,12	0,1	0,26	-0,11	0,30**	0,13
	Φ max			-0,1	0,14	-0,04	0,21	-0,1	-0,07
	Q3 Rn soil				0,33**	0,13	-0,15	0,13	0,02
	RP					0,06	0,19	0,1	0,04
	CO$_2$						0,01	0,51**	0,29**
	Temp.							-0,51	-0,02
	RH								0,27**
	Energy								

Using the non-parametric Mann-Whitney test, a statistically significant difference was found between the median radon exhalation rates in the presence and absence of concrete screed, with the absence resulting in a substantially higher median of 63 Bq/m^2/h than 25 Bq/m^2/h. The wooden ceiling led to a much higher radon exhalation rate from the floor than the concrete ceiling, which can be attributed to the chimney effect caused by the pressure difference between within and outside, which was increased by the lack of a sealed roof. With the control variable represented by the presence of concrete screed, the partial correlation coefficient between radon exhalation rate and ceiling type decreased from $r = 0,26$ ($p = 0,03$) to $r = 0,14$ ($p > 0,05$), indicating that concrete screed may have a mediating effect on the impact of ceiling type on exhalation rate. On the other hand, an association between ceiling type and indoor radon levels was not statistically significant ($p > 0,05$). In order to investigate the impact of all measured parameters on the mean indoor radon value, the multivariate linear regression method was applied, with the result that only 15 % of the variability of residential radon concentrations can be explained, with the presence of concrete screed and humidity being the primary contributors.

In conclusion, based on the analyzed data, it appears that, for the majority of study sites, the geological subsoil can provide a reasonable explanation for both the mean and high values recorded in the soil measurements (radon index and potential) and the values recorded indoors by passive measurements (which in all cases exceed the 250 Bq/m^3/year limit). The variance of residential radon could not be directly associated with the variation of radon in the soil, as this was mostly controlled by factors relating to the construction characteristics of the dwellings. It may be concluded that, in addition to geology, factors related to construction characteristics and use of dwellings have a determining role in indoor radon variation.

Chapter 4: Case study – Cluj-Napoca

In order to more precisely characterize the role of geology in the radon issue, we limited the study region to the city of Cluj-Napoca and its surrounding area. At this point in the investigation, it was possible to determine that the source of radon indoors for all residences included in the study is the soil beneath or around the foundation. It is well known that soils closely reflect the mineralogical characteristics of the parent rocks from which they form.

In terms of geological and soil influence, the indoor radon concentration data for 272 dwellings participating in the SMART-RAD-EN project in the city of Cluj-Napoca were analyzed. In addition, we followed three longitudinal trajectories from west to east, traversing the majority of geological formations and soil types in the municipality's surroundings, resulting in a total of 142 soil radon measurements. During the diagnostic phase of the SMART-RAD-EN project, when the radon potential of each residence participating in the study was evaluated, 39 soil samples were measured. The latter were measured using the RM-2 instrument, the Neznal method in 15 points, and the Radon-Jok permeameter was used to determine the permeability. From a total of 15 measurement points, three were chosen at random to provide data for the geo-pedological trajectories. Each of the other 103 soil measurements were taken at three points (at the ends of an equidistant triangle grid with 1 m sides) using the LUK 3P instrument and the Bottle permeameter to determine permeability.

Geological and pedological attributes were attributed to each individual measurement using Q-Gis software and geological and pedological maps (1:200,000). Excel was used to create the database, while IBM SPSS Statistics 20 was utilized for statistical analysis. The existing literature was used to compile a summary of the geology and pedology of the research region.

4.1. Geology and pedology of Cluj-Napoca municipality and peri-urban area

From a geological point of view, the municipality of Cluj-Napoca is located in the northwestern part of the Transylvanian Basin, to the east of the metamorphites of the Gilău Mountains, in the region which, in the literature, is called the "Gilău area", at the level of the distribution of Paleogene sedimentary facies (Rusu, 1970). The region is characterized by a diversity of geological formations and structures, with metamorphic, magmatic and sedimentary rocks of different ages and petrographic types (Krézsek, 2006, and references therein).

Formations of Upper Cretaceous age are found above the metamorphic and eruptive rocks, over which are discordantly transgressive Palaeogene and Neogene formations, predominantly detrital, carbonate or volcanogenic-sedimentary in character (Figure 8). They correspond to distinct sedimentary basins in terms of overlying roles and evolution.
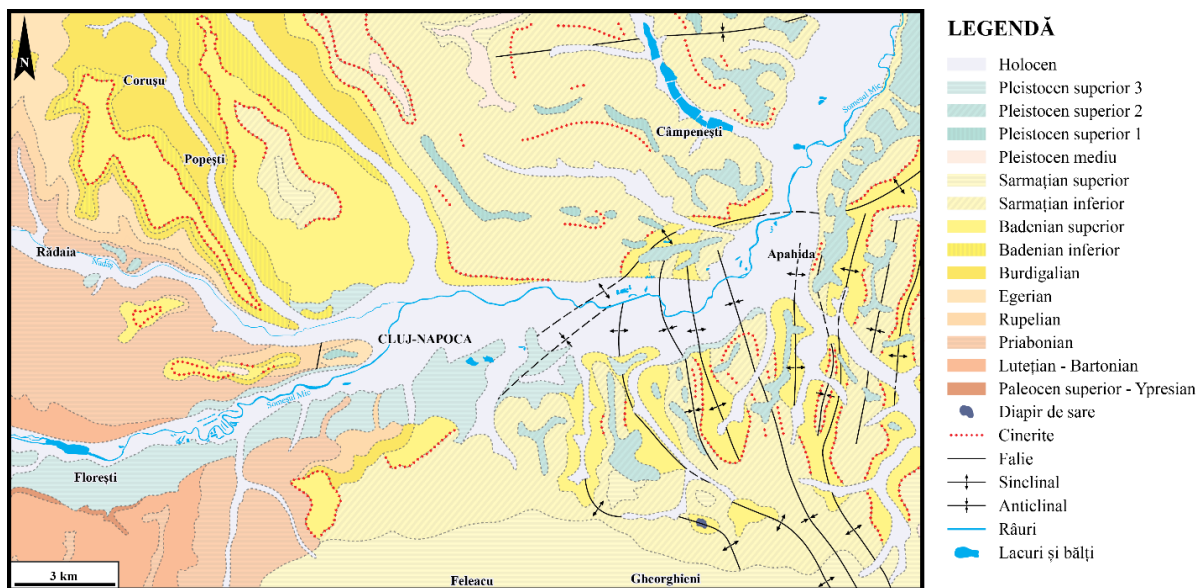
Figure 8. Geological map of Cluj-Napoca region [modified after Răileanu and Saulea (1967); hydrography after maps.google.com].

4.1.1. *Stratigraphy*

I.   *Metamorphic basement and overlaying sedimentary formations*

The oldest rocks are represented by crystalline schists that formed during the Precambrian, in the region where the Gilău massif was subsequently built. These are mainly metamorphic rocks of Paleozoic age (Someș Series and Arada Series) (Săndulescu and Visarion, 1978; Săndulescu, 1988; = Someș Lithogroup in Balintoni, 1997) over which a

sedimentary cover of Triassic - Upper Cretaceous age (e.g., Burchfiel, 1976; Paraschiv, 1979; Krézsek and Bally, 2006). This whole assemblage belongs to the Bihor Unit (Săndulescu, 1984), also known as the " Autochthon of Bihor " (Mutihac and Ionesi, 1974).

II.   Upper Cretaceous

The closest deposits of terminal Cretaceous age to the municipality of Cluj-Napoca are located in the inner Dacidae, between Gilău and Someşul Rece, or in other areas (Stolnei, Sărăţii, Someşului Mic and Agârbiciu) (Mészáros and Clichici, 1976; Baciu and Filipescu, 2002; Săsăran and Săsăran, 2003; Săsăran, 2011). They depict the tachygenesis processes that happened at the end of the Cretaceous in the Northern Apennines (Săndulescu, 1984). These are deposits with a flixoid appearance, with a narrow and deep tectonic basin, but which in the early stages of evolution, or later exclusively on the margins of the basin, permitted the development of the Gosau-type facies, with all of the abundant mollusk fauna characteristic of this facies. They should not be confused with the Transylvanian flixoid deposits located further south (region of Hăşdate), with the facies reported by Săsăran and Săsăran (2003).

Magmatic activity at the end of the Cretaceous, associated with "Laramic" movements, determines the emplacement of eruptive rocks belonging to banatites (dacite, andesite and rhyolite) in the valleys of Căpuş, Someşul Rece, in the Mănăstireni or Băişoara-Săcel area (Vlaicu-Tătărâm, 1963; Ștefan et al., 1985). The most important contributions on the genesis of magmatic rocks in the area are those of Hanomolo and Hanomolo (1962), Vlaicu-Tătărâm (1963), Mureşan (1974; 1980), Lazăr and Întorsureanu (1982), Ștefan et al. (1985; 1988; 1992).

III.   Paleogene

Paleogene deposits in the northwestern portion of the Transylvanian Basin include the fill of a foreland basin characterized by "Laramic" tectogenesis (Hosu, 1999; Fărcaş, 2011). The thickness of the deposits ranges from 500 m in the northwestern portion of the Transylvanian Basin to over 1800 m in the Jibou-Preluca area to the north, where continental and marine facies layers alternate vertically (e.g., Popescu, 1984; Hosu, 1999; Filipescu, 2011).

IV.   Neogene

The series of Neogene deposits starts with the establishment of the Coruşu Formation (Acvitanian-Lower Burdigalian) during a transgression. This is preceded by the Chechiş Formation and the Hida Formation, both of which show a regression; the latter is also defined by fluvial-deltaic facies, with which the Lower Miocene sedimentation cycle of the

Transylvanian Basin concludes (Mészáros and Clichici, 1976; Filipescu, 2011). The Middle Miocene begins with a sequence of dacitic tuffs and marls from the Dej Formation, which is followed by an evaporite sequence including gypsum and salt from the Ocna Dejului Formation. Another series of tuffs (Volhinian) can be discovered in the Iris Formation, which also marks the ending of the saline depositional trends. The Feleac Formation closes the Middle Sarmatian sedimentation cycle with its regressive nature (Mészáros and Clichici, 1976).

V. Quaternary

Erosion and accretion processes specific to this epoch gave rise to Pleistocene and Holocene fluvial terrace and meadow deposits, mainly composed of gravels and sands. These are specific to present-day valleys and their tributaries.

4.1.2. Pedology

The soil in the peri-urban area of Cluj-Napoca, which is typical of agricultural and forested areas, is diverse and tightly linked to geomorphological, geological, and environmental elements, being directly affected by relief, rock, climate, and vegetation. In urban areas, where soils have been substantially altered by humans and cannot be termed soil *per se*, the situation is very different (Figure 9).
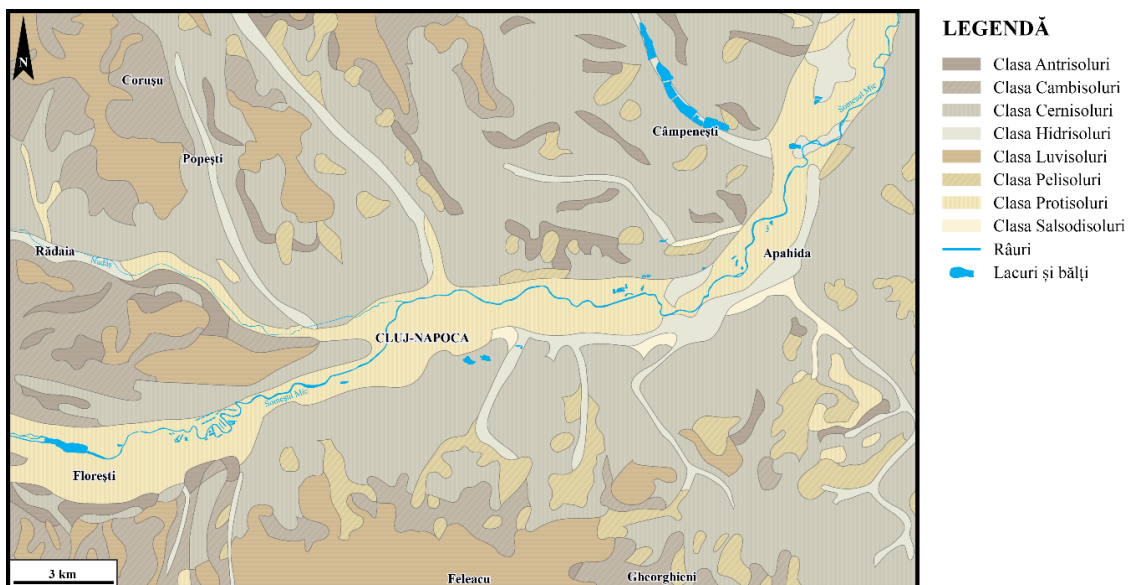
Figure 9. Map illustrating the restricted soil classes for the region of study [modified after Florea and Asvadurov (1994); hydrography after maps.google.com].

Studies carried out in the surroundings of Cluj-Napoca municipality have revealed the presence of soils of the Chernozemic Class (represented by cambic chernozomes, clayey silty

chernozomes, pseudorendzines, rendzines and faeozomes), Luvisolic Class (prelvosols and luvosols), Hydrisolic Class (represented by stagnosols and gleisols), Salsodisols Class (represented by solonceacts and solonites), Protisols Class (represented by alluvial soils), Antrisols Class (represented by erodisols), Pelisols Class (represented by vertosols) and Cambisols Class (represented by eutricambosols) (Piciu et al. , 2002) (Figure 9).

4.2. Summary statistics

The 272 indoor radon concentration measurements are represented by the annual average of the values from the two measurement campaigns of the SMART-RAD-EN project. The soil radon measurements on geological trails are represented by the arithmetic mean of the radon concentration values measured at the three points for each location. Also, since permeability has been established for each point, it is further represented as either the arithmetic mean (Permeability), geometric mean (G.M. Permeability) or median (Median Permeability) of the 3 measurements for each location. Furthermore, for the soil measurements, the data were also analysed in terms of the Neznal (P.R. and R.I Neznal) and Kemski (R.I. Kemski) radon potential and index, as well as the radon concentration expressed as its arithmetic mean (CRn in soil), geometric mean (M.Geom. CRn) and median (Median CRn) for each location. In addition, a radon potential (Geom.M. potential) was calculated by logarithmizing the radon concentration expressed by the geometric mean. Descriptive statistics of indoor and soil sample radon measurements are shown in Table 5, where AM is the arithmetic mean, SD is the standard deviation, GM is the geometric mean and Med. is the median.

As can be seen from Table 5, in terms of annual average indoor radon concentration (indoor CRn), minimums of 10 Bq/m^3 and maximums of 1221 Bq/m^3 were measured. The arithmetic mean and geometric mean are 148 and 102 Bq/m^3 respectively, and the median is 91 Bq/m^3.

In terms of soil radon concentration, represented by the arithmetic mean of the values measured at 3 sampling points, minimum values of 4,3 kBq/m^3 and maximum values of 77,7 kBq/m^3 were recorded, with arithmetic and geometric means of 25,8 and 22,7 kBq/m^3 respectively, the median being drawn at 24,2 kBq/m^3. The radon concentration represented by the geometric mean (M. Geom. CRn) showed similar values, with minima and maxima of 4,3 and 77,6 kBq/m^3 respectively, an arithmetic and geometric mean of 25,2 and 22 kBq/m^3 respectively and the median plotted at 23,4 kBq/m^3. Similar values were found for the radon concentration in the soil expressed as the median of the values measured at the three points,

28

with minimum and maximum values of 5,5 and 78,6 kBq/m^3 respectively, with arithmetic and geometric means of 25,5 and 22,3 kBq/m^3 respectively and the median plotted around 23,4 kBq/m^3. In contrast, as expected, the radon concentration expressed as the potential of the geometric mean of the radon concentration showed lows and highs of 2 and 108,8 kBq/m^3 respectively, with arithmetic and geometric means of 18,8 and 15 kBq/m^3 respectively and a median plotted at 16,6 kBq/m^3.

Table 5. Summary statistics for indoor and soil radon measurements for Cluj-Napoca.

Type of measurment	Total nr.	Min.	Max.	A.M.	S.D.	G.M	Med.
Indoor CRn (kBq/m^3)	272	10	1221	148	152	102	91
Soil CRn (kBq/m^3)		5,2	77,7	25,8	13,3	22,7	24,2
M.Geom.CRn		4,3	77,6	25,2	13,1	22	23,4
Median CRn		5,5	78,6	25,5	13,6	22,3	23,4
Potential from M.Geom.		2,2	108,8	18,8	14,4	15	16,6
Permeability		$1,58 \cdot 10^{-13}$	$5,02 \cdot 10^{-11}$	$9,21 \cdot 10^{-12}$	$1,04 \cdot 10^{-11}$	$4,75 \cdot 10^{-12}$	$5,68 \cdot 10^{-12}$
M.G. permeability		$1,58 \cdot 10^{-13}$	$4,83 \cdot 10^{-11}$	$6,14 \cdot 10^{-12}$	$7,64 \cdot 10^{-12}$	$3,08 \cdot 10^{-12}$	$3,93 \cdot 10^{-12}$
Permeability median		$1,57 \cdot 10^{-13}$	$4,9 \cdot 10^{-11}$	$7,43 \cdot 10^{-12}$	$9,79 \cdot 10^{-12}$	$3,03 \cdot 10^{-12}$	$4,03 \cdot 10^{-12}$
R.P. Neznal		2	146				22
R.I. Neznal		Low	Median	High			
		23	93	23			
P.R. Kemski		Level 1	Level 2	Level 3	Level 4		
		10	18	64	59		

The mean permeability of the three test points for each location showed minimum values of 1,58-10-13 and maximum values of 5,02-10-11, with arithmetic and geometric means of 9,21-10-12, respectively 4,75-10-12 and a median of 5,68-10-12.

In terms of Neznal radon potential, there was a minimum potential of 2 and a maximum of 146, with a median potential of 22. Also, in terms of the Neznal radon index, there were 23 values with low index, 93 with medium index and 23 with high index.

In terms of the Kemski radon potential, 10 measurements are classified in risk level 1, 18 in level 2, 64 in level 3 and 59 in level 4.

Chapter 5: Results

5.1. Analysis of residential radon measurements in relation to the area's geology and pedology

The 272 indoor radon measurements reflect the same number of locations, which overlap 12 soil types that have been subdivided into 9 classes for the purpose of a more accurate statistical analysis. Protisols Class (Proti.), Cambisols Class (Camb.), Chernisols Class (Cern.),

Hydrisols Class (Hidr.), Luvisols Class (Luv.), Pelisols Class (Peli.), Salsodisols Class (Sals.). Geologically, the 272 places overlap 12 geological deposits determined by age, which were subsequently classified into geological epochs for the same statistical purpose. In the Eocene (Eoc.), we included the Lutetian and Priabonian, in the Oligocene (Olg.), we included the Kiscelian, in the Oligocene-Miocene (OlgMc.), we included the Aegerian, in the Miocene (Mc.), we included the Eggerian - Ottnagian, Badenian, and Sarmatian. Table 6 and Figure 10 illustrate the frequency of measurements for each geological age and soil type, respectively.

Table 6. Frequency of indoor radon measurements specific to each geological age and soil class.

GEOLOGY	Frequency	Ratio (%)	PEDOLOGY	Frequency	Ratio (%)
Hol.	89	32,7	Camb.	9	3,3
Pl.	85	31,5	Cern.	125	46
Mc.	64	23,5	Hidr.	23	8,5
OlgMc.	10	3,7	Luv.	19	7
Olg.	17	6,3	Peli.	8	2,9
Eoc.	7	2,6	Proti.	85	31,3
			Sals.	3	1,1
Total	272				

The Kruskal-Wallis non-parametric independent samples test was applied for residential radon concentration as a function of geology and pedology. The significance level was chosen at 0.05. For soil classes there is no statistically significant difference (p = 0,054), but for geological ages there is a statistically significant difference (p < 0,05), namely between Oligocene and Holocene (Olg-Hol.) (p = 0,025), Oligocene and Pleistocene (Olg.- Pl.) (p = 0,008), Miocene and Holocene (Mc-Hol.) (p = 0,026), Miocene and Pleistocene (Mc.-Pl.) (p = 0,004), as shown by Dunn's post-hoc test. Figure 11 shows the comparison diagram between the pairs involved.

To normalize the data distribution, residential radon values were logarithmed. By applying the one-way Anova test, the interaction between GEOLOGY and PEDOLOGY variables on residential radon expressed as logarithm of the annual mean was followed, which showed a statistically significant impact for the interaction between geological epochs and soil classes (p = 0,013).

By calculating the Pearson correlation coefficient, an acceptable correlation was obtained between GEOLOGY and PEDOLOGY (r = - 0,141, p < 0,05). In contrast, no statistically significant correlation was obtained between the variables GEOLOGY and PEDOLOGY and residential radon concentration (p > 0,05).
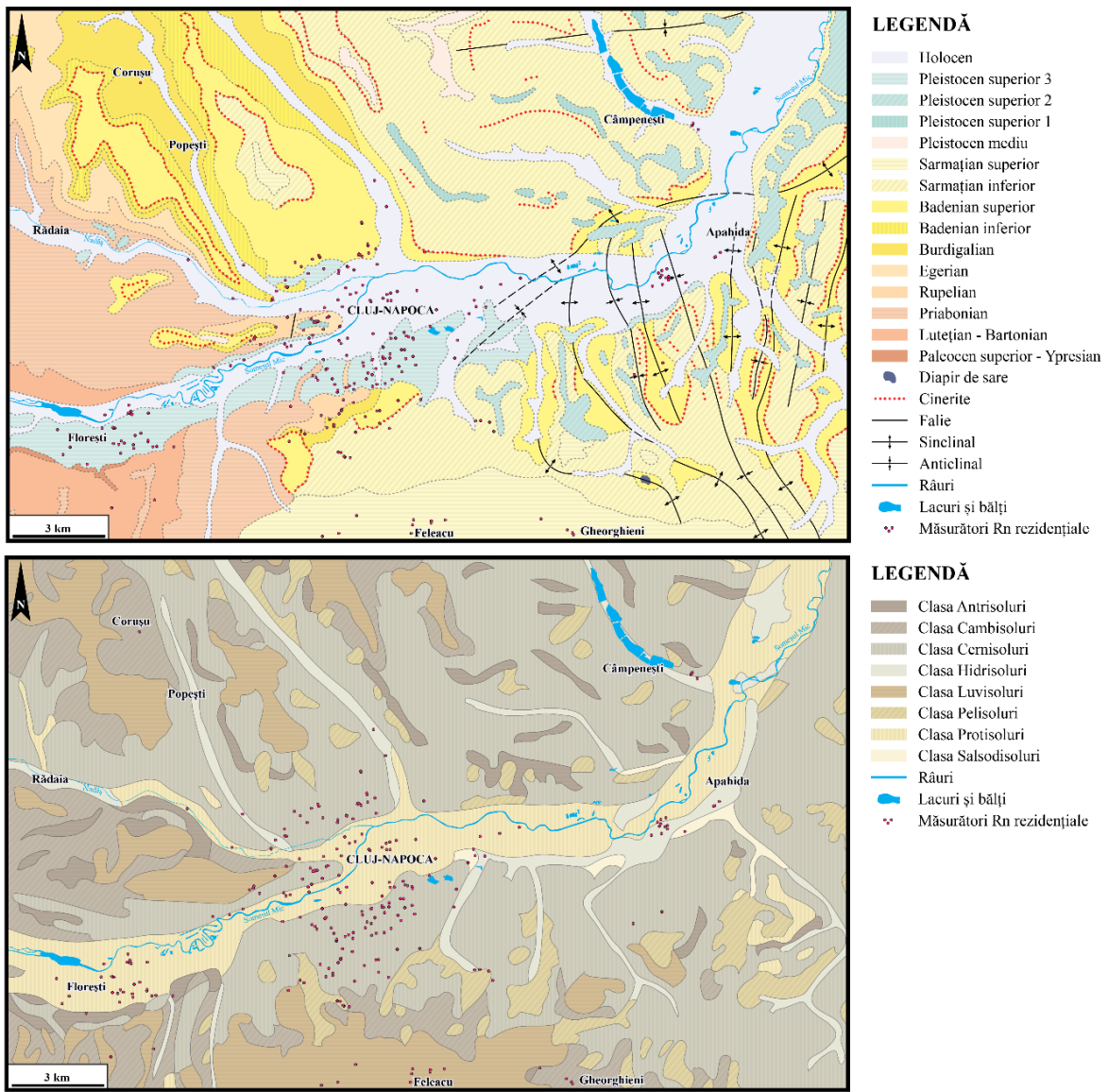
Figure 10. Distribution of residential measurement points according to geology and pedology [modified after Răileanu and Saulea (1967), Florea and Asvadurov (1994); hydrography after maps.google.com]
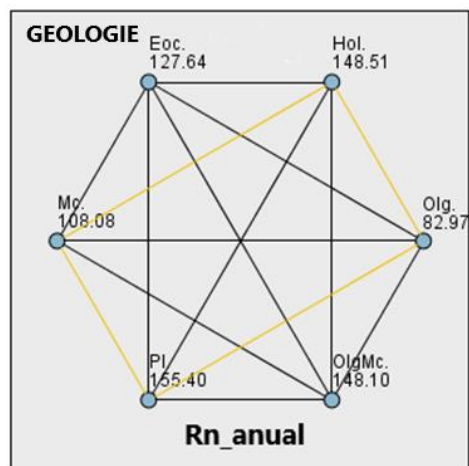
Figure 11. Geology as a function of annual radon concentrations, plotted using pairwise comparisons.

31

5.2. Analysis of soil radon measurements in relation to the geology and pedology of the area

In the case of soil measurements, the division of crossed geological and pedological formations was also restricted to geological epochs and soil classes. All geological epochs and soil classes from the residential measurements were intercepted through the three geological tracts, in addition to which an additional class represented by the Antrisols Class (Antr.) was intercepted. Figure 12 shows the frequency of measurements for each geological epoch and soil class.
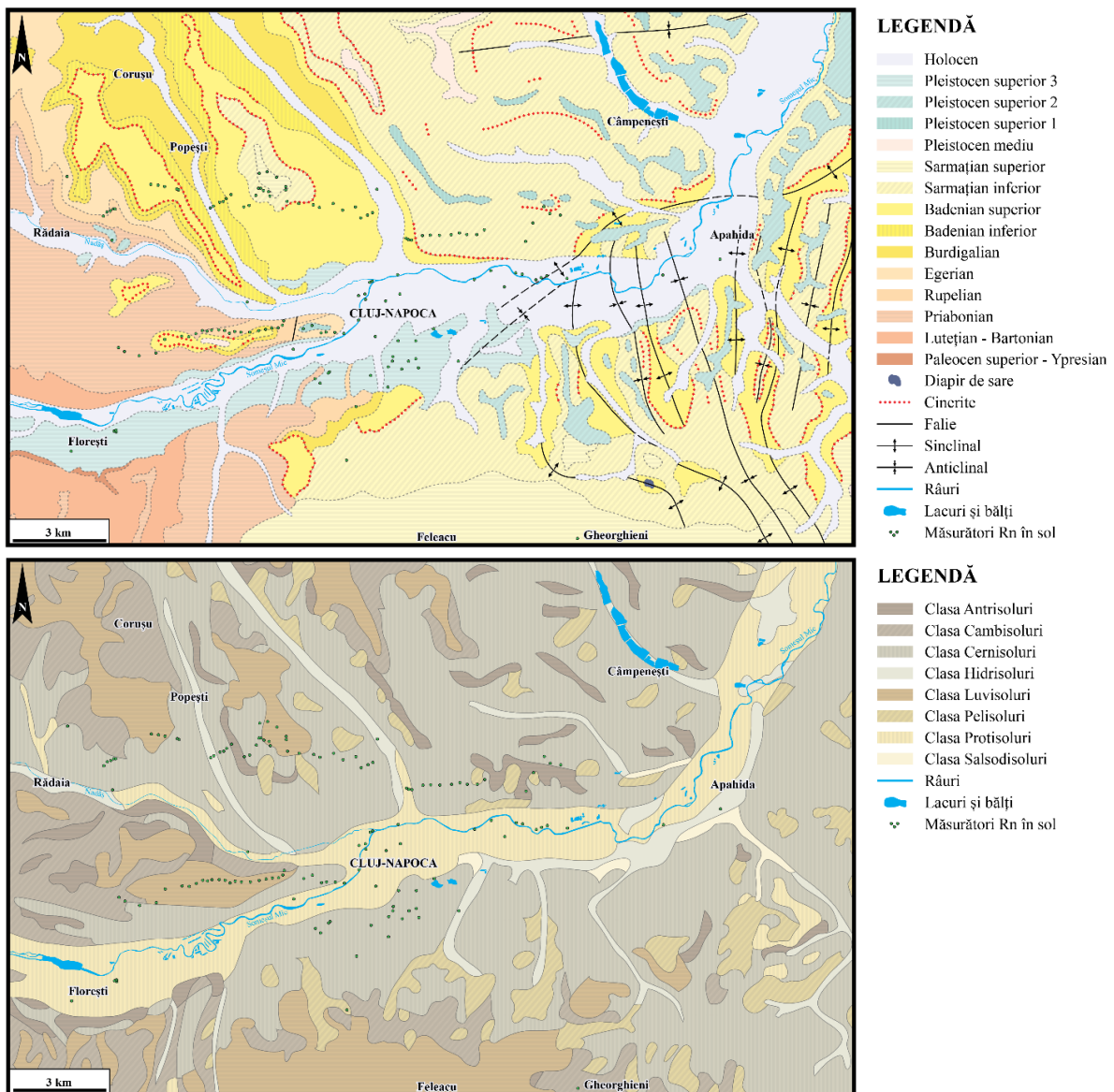
Figure 12. Distribution of soil measurement points according to geology and pedology [modified after Răileanu and Saulea (1967), Florea and Asvadurov (1994); hydrography after maps.google.com].

32

Most of the soil measurements were taken where underlying Miocene deposits are present, with a share of 39,4 %. The Holocene and Pleistocene have a share of 19 and 18,3 % respectively, followed in order of frequency by Oligocene (9,2 %), Eocene (8,5 %) and Oligocene-Miocene (5,6 %).

From a pedological point of view, the Chernisols have the highest frequency in terms of soil classes in which radon measurements have been carried out, with a share of 41,5 %, followed, in order of frequency, by Protisols and Luvisols with a share of 23,2 % and 21,1 % respectively. Much less radon soil measurements were intercepted in Cambisols (6,3 %), Antrisols (2,8 %) and Hydrisols (2,8 %).

As regards the raw values of radon concentration measured in soil gas on geological tracts, expressed by arithmetic mean (A.M.), geometric mean (G.M.) and median (Med.), in this case, as in the case of residential measurements, the maximum values were recorded, within geological epochs, in the Pleistocene, and in the case of soil classes, by the Chernobyls, with 77 kBq/m^3. In terms of minimum and maximum values, the proportions are mostly preserved for all three representations, with the Oligocene-Miocene following in descending order of maximum values. The Holocene shows higher maxima for the arithmetic mean and geometric mean data representations than the Eocene but in terms of median, the maximum for the Eocene is higher than the Holocene.

The non-parametric Kruskal-Wallis test applied to determine the impact of GEOLOGY and PEDOLOGY variables on radon concentration, expressed as geometric mean and median, showed statistically significant differences for both geological ages and soil classes ($p < 0,05$).

For radon in soil expressed by geometric mean, statistically significant differences were observed for GEOLOGY for the Holocene and Pleistocene ($p = 0,000$), Holocene and Oligocene-Miocene ($p = 0,006$), Eocene and Pleistocene ($p = 0,039$), and Miocene and Pleistocene data pairs, respectively, and for PEDOLOGY only one statistically significant difference, for the Protisols and Chernisols pair ($p = 0,027$), as shown by Dunn's post hoc test.

For radon in soil expressed by median, statistically significant differences were observed for GEOLOGY, and Dunn's post hoc test showed differences for Holocene and Oligocene-Miocene ($p = 0,009$), Holocene and Pleistocene ($p = 0,000$), Miocene and Pleistocene ($p = 0,006$) data pairs, and for GEOLOGY only a statistically significant difference for Protisols and Chernisols ($p = 0,028$). Figure 13 shows the comparison plots between pairs.

For normalizing the data distribution, the soil radon concentration values, expressed by geometric mean, were logarithmed. Kolmogorov-Smirnov (p = 0,200) and Shapiro-Wilk (p = 0,118) normality tests showed that logarithmizing the data resulted in a log-normal distribution.
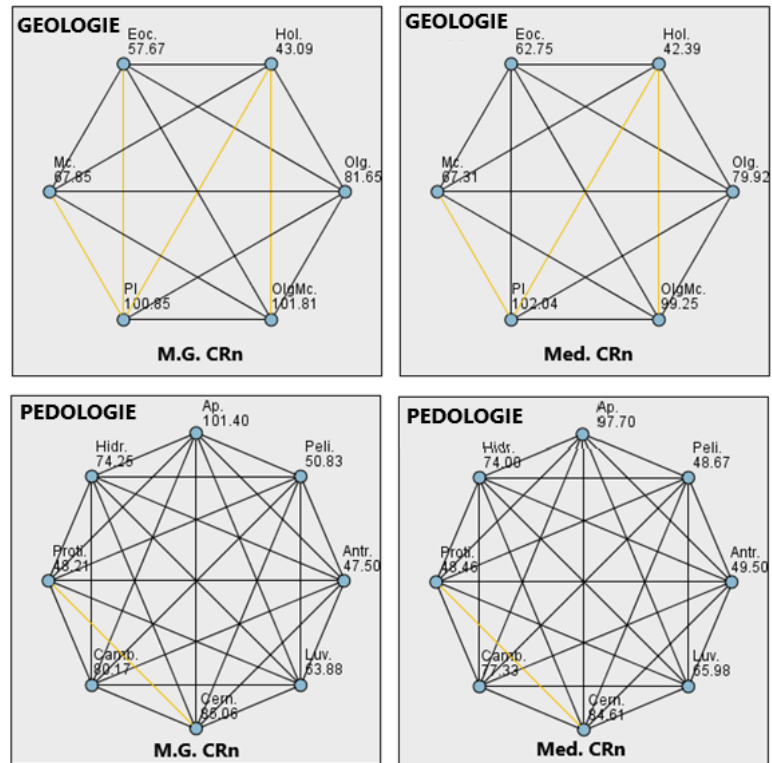
Figure 13. Comparison diagrams between pairs of data of each variable (geology and pedology) according to the geometric mean radon concentration (M.G.CRn) and its median (Med.CRn).

By applying the parametric one-way ANOVA test, the impact of the variables GEOLOGY and PEDOLOGY on radon in the soil, expressed as logarithm of the geometric mean, along with the interaction between the two variables was investigated. For the variables GEOLOGY and PEDOLOGY a statistically significant difference was observed between geological ages (p < 0,05) on the one hand and between soil classes (p < 0,05) on the other hand. Tukey's poc-hoc test revealed a statistically significant difference for Holocene and Pleistocene (p = 0,021), Holocene and Oligocene-Miocene (p = 0,003), Eocene and Pleistocene (p = 0,018), Miocene and Pleistocene (p = 0,018), and Protisols and Chernisols (p = 0,050) data pairs, respectively.

The interaction between GEOLOGY and PEDOLOGY has a statistically significant impact for the analysed dataset (p = 0,043) and GEOLOGY (p = 0,009), respectively.

If entered into a linear regression model, then the geometric mean log radon concentration will depend on both variables (GEOLOGY and PEDOLOGY). The adjusted coefficient of determination for this model is 0,16 (low).

Permeability was calculated as the geometric mean of the values measured at the three points in the soil, but for a better descriptive evaluation it was chosen to divide its values into three permeability categories, following the Neznal et al. (Thus, the three categories are low permeability ($k < 4,0 \cdot 10^{-13}/$ m^2), medium permeability ($4,0 \cdot 10^{-13} < k < 4,0 \cdot 10^{-12}/$ m^2) and high permeability ($k > 4,0 \cdot 10^{-12}/$ m^2) (Table 7).

Table 7. contingency table for permeability categories and soil classes.

Permeability categories	PEDOLOGY							Total
	Antr.	Camb.	Cern.	Hidr.	Luv.	Peli.	Proti.	
Low	1	2	3	0	5	1	1	13
Medium	0	4	32	3	13	1	7	60
High	3	3	24	1	12	1	25	69
Total	4	9	59	4	30	3	33	142

As can be seen in contingency table 7, out of a total of 142 soil measurements, 69 measurements showed a high permeability value, with a share of 48,59 %. Another 60 measurements showed a medium permeability value, with a share of 42,25 % of the total. Only 13 measurements showed low permeability values, representing only 9,15 % of the total.

The non-parametric Kruskal-Wallis test applied to determine the impact of the variables GEOLOGY and PEDOLOGY on permeability, expressed by the geometric mean of permeability, showed a statistically significant difference for both variables ($p < 0,05$), for the Eocene and Holocene ($p = 0.037$), Luvisols and Protisols ($p = 0,003$) and Chernisols and Protisols ($p = 0,013$) pairs, respectively, as revealed by Dunn's post hoc test (Figure 14). For the permeability classes, no statistically significant difference was observed for any of the variables GEOLOGY or PEDOLOGY ($p > 0,05$). The significance threshold α was set at 0,05 with a 95 % confidence interval.

Along with radon concentration and permeability, the relationship between the two was considered in the form of radon potential. A radon potential was calculated according to the method of Neznal et al. (2004) adapted for 3 points - to which we added the Neznal radon index, another according to the method of Kemski et al. (2004) and a third potential calculated

according to the geometric mean of radon concentration in relation to the geometric mean of permeability (Potential from M.G.).
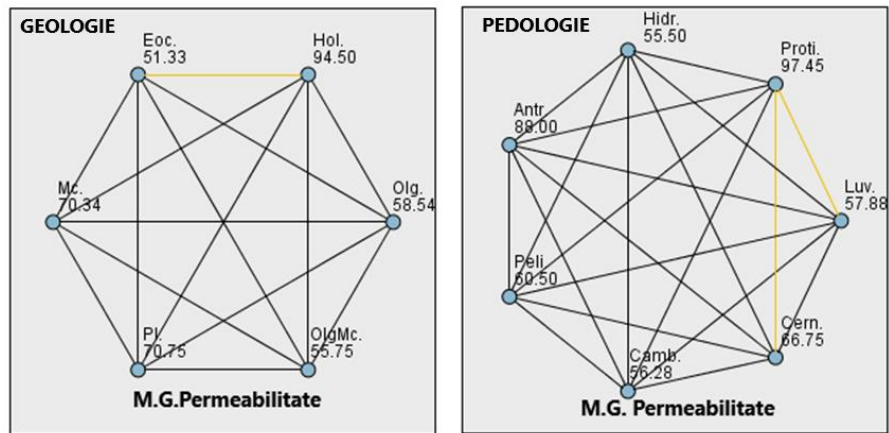
Figure 14. Comparison diagrams between data pairs of each variable (geology and pedology) according to permeability (M.G. Permeability).

The Kruskal-Wallis non-parametric test applied to determine the impact of the GEOLOGY and PEDOLOGY variables on the Neznal radon potential showed a statistically significant difference only for the GEOLOGY variable ($p < 0{,}05$) - for the Holocene and Pleistocene ($p = 0{,}001$), Eocene and Pleistocene ($p = 0{,}027$) and Miocene and Pleistocene ($p = 0{,}033$) pairs. Similarly, for the geometric mean radon potential a statistically significant difference is observed only for the variable GEOLOGY ($p < 0{,}05$) - for the Eocene and Pleistocene ($p = 0{,}007$), Holocene and Pleistocene ($p = 0{,}041$) pairs, as shown by Dunn's post-hoc test (Figure 15). The significance threshold α was set at 0.05, with a 95 % confidence interval.
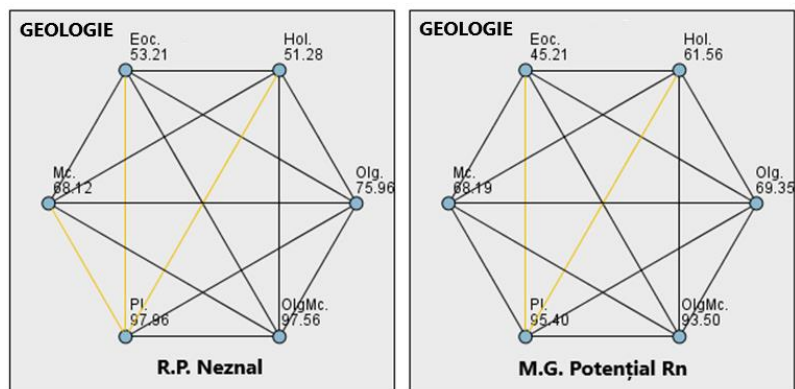
Figure 15. Comparison plots of data pairs of the variable geology versus Neznal Radon Potential (Neznal R.P.) and geometric mean potential of radon concentration in soil (M.G. Potential Rn).

To normalize the data distribution, the values of the geometric mean potential as well as the Neznal potential were logarithmed. Kolmogorov-Smirnov and Shapiro-Wilk normality tests revealed that logarithmizing the data resulted in a log-normal distribution for both data sets ($p > 0,05$).

By applying the parametric one-way ANOVA test, the impact of the variables, separately for GEOLOGY and PEDOLOGY, on the logarithmically expressed Neznal radon potential and the logarithmically expressed potential from the geometric mean, for each set of values, was investigated. For the GEOLOGY and PEDOLOGY variables, a statistically significant difference was observed only between geological epochs ($p < 0,05$). The Tukey poc-hoc test revealed a statistically significant difference for Holocene and Pleistocene ($p = 0,000$), Holocene and Oligocene-Miocene ($p = 0,003$), Eocene and Pleistocene ($p = 0,018$), Eocene-Oligocene-Miocene ($p = 0,036$), Eocene and Pleistocene ($p = 0, 011$) for radon potential expressed by geometric mean, respectively between Pleistocene and Eocene ($p = 0,023$), Pleistocene and Holocene ($p = 0,001$), Pleistocene and Miocene ($p = 0,031$), Holocene and Oligocene-Miocene ($p = 0,026$) in terms of Neznal radon potential.

If entered into a linear regression model, then the logarithmic mean values of the geometric mean radon concentration and the Neznal radon potential will depend only on the GEOLOGY.

Following the methods presented in Chapter 2, the Kemski Radon Potential (Kemski R.P.) and the Neznal Radon Index (Neznal R.I.) were calculated for each location where soil measurements were made. The Neznal Radon Index is divided into 3 categories (low, medium, high), which represent the radon risk for a site to be built or already built. The Kemski radon potential is divided into 6 classes representing the potential for geogenic radon generation. A value of 1 means the lowest potential and a value of 6 indicates the highest potential. In contingency tables it can be seen that in the case of the Neznal radon index all three classes were covered by measurements. In contrast, in the case of the Kemski geogenic radon potential only the first four categories were covered.

In terms of the Neznal radon index, out of a total of 142 soil measurements, there were 23 low indexes (16,2 %), 93 medium indexes (65,49 %) and 26 high indexes (18,31 %).

The Kruskal-Wallis non-parametric test applied to determine the impact of GEOLOGY and PEDOLOGY variables on the Neznal radon index showed a statistically significant

difference only for the GEOLOGY variable (p < 0,05), for the Holocene and Pleistocene pair (p = 0,015) (Figure 16).
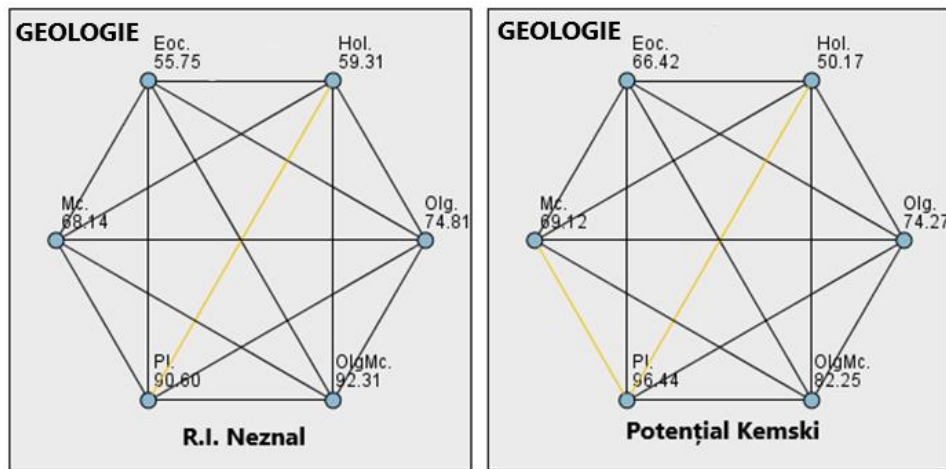
Figure 16. Comparison plots between pairs of data of the variable geology as a function of (R.P. Neznal) and the geometric mean potential of radon concentration in soil (M.G. Potential Rn).

The Kruskal-Wallis non-parametric test applied to determine the impact of GEOLOGY and PEDOLOGY variables on Kemski geogenic radon potential showed a statistically significant difference only for the GEOLOGY variable (p < 0,05), for the Holocene and Pleistocene pairs (p < 0.001), and for the Miocene and Pleistocene (p = 0,033) (see Figure 16).

By calculating the Pearson correlation coefficient, an acceptable correlation was obtained between GEOLOGY and soil radon concentration expressed by M.G. CRn (r = 0,409, p < 0,01) and Med. CRn (r = 0,415, p < 0,01), also between GEOLOGY and M.G. Potential Rn (r = 0,330, p < 0,01) Geogenic Radon Potential Kemski (r = 0,344, p < 0,01), Neznal Potential (r = 0,381, p < 0,01) and Neznal Radon Index (r = 0,344, p < 0. An inverse correlation was obtained for the interaction between GEOLOGY and PEDOLOGY (r = - 0,206, p < 0,05). No statistically significant correlation was observed between GEOLOGY and permeability as well as permeability class. For PEDOLOGY, a statistically significant correlation was obtained for permeability expressed by geometric mean (r = 0,193, p < 0,05) as well as permeability class (r = 0,184, p < 0,05). An inverse correlation was obtained between PEDOLOGY and radon concentration measured in soil, expressed by geometric mean (r = -0,197, p < 0,05), including median (r = -0,206, p < 0,05) (Table 8).

Table 8. Statistical correlations determined for measured parameters; **correlation is significant at 0,01 level; *correlation is significant at 0,05 level.

Pearson Correlation	M.G. CRn	Med. CRn	M.G. Potential Rn	R.P. Kemski	R.P. Neznal	R.I. Neznal	Class perm.	M.G. perm.	GEO.	PEDO.
M.G. CRn	X	0,980**	0,789**	0,650**	0,707**	0,585**	-0,104	-0,114	0,409**	-0,197*
Med. CRn	0,980**	X	0,778**	0,636**	0,708**	0,604**	-0,095	-0,103	0,415**	-0,206*
M.G. Potential Rn	0,789**	0,778**	X	0,587	0,858**	0,761**	0,414**	0,496**	0,330**	-0,61
R.P. Kemski	0,650**	0,636**	0,587**	X	0,746**	0,672**	0,053	0,077	0,344**	-0,094
R.P. Neznal	0,707**	0,708**	0,858**	0,746**	X	0,890**	0,304**	0,392**	0,381**	-0,084
R.I. Neznal	0,585**	0,604**	0,761**	0,672**	0,890**	X	0,329**	0,423**0	0,344**	-0,051
Clasă perm.	-0,104	-0,095	0,414**	0,053	0,304**	0,329**	X	0,892**	-0,057	0,184*
M.G. perm.	-0,114	-0,103	0,496**	0,077	0,392**	0,423**	0,892**	X	-0,034	0,193*
GEOLOGIE	0,409**	0,415**	0,330**	0,344**	0,381**	0,344**	-0,057	-0,034	X	-0,206*
PEDOLOGIE	-0,197*	-0,206*	-0,061	-0,094	-0,084	-0,051	0,184*	0,193*	-0,206*	X

5.3. Combined analysis of residential and soil radon measurements in relation to the geology and pedology of the area

At the level of Cluj-Napoca municipality, out of a total of 272 residential radon measurements, there were 34 measurements exceeding the reference level of 300 Bq/m^3. Of the 34 locations, only 24 were diagnosed (Table 9), according to the availability of the owners. For each location, out of the total of 15 soil measurement points, three points were chosen close to each other and the potential was recalculated based on radon concentration and permeability values.

The measurements covered formations that corresponded for only 3 geological epochs. The Pleistocene had the most measurements (17) with a share of 70 % of the total, followed by the Holocene (6) with a share of 25 % of the measurements. The Miocene had only one measurement which accounted for 4,2 % of the total. From a pedological point of view, the measurements overlapped over 3 soil classes. Chenisols, with 12 measurements, had the highest share of the total (50 %), followed by Protisols with 11 measurements (45,9 %) and Hydrisols with only one measurement (4,2 %).

By calculating the Pearson correlation coefficient, for all variables, no statistically significant correlation was obtained between residential radon concentration and any of the variables, the only exception being permeability (r = 0,420, p < 0,05). In contrast, statistically significant correlations were observed from all crosses of the variables resulting from soil radon

concentration (Geometric Mean, Kemski Potential, Potential and Neznal Radon Index) (p < 0,01), which is natural given that they are based on the same set of values. A statistically significant correlation was also obtained between the variable GEOLOGY and the geometric mean radon concentration (r = 0,697, p < 0,01), the Neznal Radon Potential (r = 0, 567, p < 0,01) , Neznal Radon Index (r = 0,653, p < 0,01) and Kemski Potential (r = 0,749, p < 0,01) as well as for the geometric mean radon potential (r = 0,464, p < 0,05). No statistically significant correlation was obtained for the PEDOLOGY variable (p > 0,05). Table 10 shows the summary of statistical correlations for the measured parameters.

Table 9. Summary statistics for residences exceeding 300 Bq/m3 where diagnosis was performed.

Nr.	CRn_annual (Bq/m^3)	M.G. CRn_soil (kBq/m^3)	Potential from M.G. (kBq/m^3)	M.G. Perm. (k/m^2)	Class perm.	R.P. Neznal	R.I. Neznal	R.P. Kemski	GEO.	PEDO.
1	373	32	21	$3,13 \cdot 10^{-12}$	mediu	35	mediu	4	Pl.	Proti.
2	367	32	18	$1,69 \cdot 10^{-12}$	mediu	26	mediu	4	Pl.	Proti.
3	309	39	35	$8,16 \cdot 10^{-12}$	ridicat	44	ridicat	4	Pl.	Proti.
4	396	18	14	$6,07 \cdot 10^{-12}$	ridicat	27	mediu	3	Pl.	Proti.
5	336	37	40	$1,30 \cdot 10^{-11}$	ridicat	45	ridicat	4	Pl.	Proti.
6	326	71	50	$4,02 \cdot 10^{-12}$	ridicat	81	ridicat	4	Pl.	Proti.
7	584	16	12	$6,36 \cdot 10^{-12}$	ridicat	4	scăzut	1	Hol.	Hidr.
8	394	10	9	$1,71 \cdot 10^{-11}$	ridicat	10	scăzut	1	Hol.	Proti.
9	366	9	7	$6,36 \cdot 10^{-12}$	ridicat	2	scăzut	1	Mc.	Cern.
10	423	38	17	$6,94 \cdot 10^{-13}$	mediu	18	mediu	3	Pl.	Cern.
11	333	78	32	$4,30 \cdot 10^{-13}$	mediu	34	mediu	3	Pl.	Cern.
12	347	34	17	$1,05 \cdot 10^{-12}$	mediu	23	mediu	4	Pl.	Cern.
13	432	8	7	$1 \cdot 10^{-12}$	ridicat	5	scăzut	1	Hol.	Proti.
14	376	22	17	$5,52 \cdot 10^{-12}$	ridicat	20	mediu	3	Pl.	Cern.
15	330	15	8	$1,98 \cdot 10^{-12}$	mediu	12	mediu	3	Pl.	Cern.
16	656	19	20	$1,28 \cdot 10^{-11}$	ridicat	29	mediu	3	Hol.	Proti.
17	768	42	26	$2,78 \cdot 10^{-12}$	mediu	50	ridicat	4	Pl.	Cern.
18	531	17	17	$1,08 \cdot 10^{-12}$	ridicat	27	mediu	3	Hol.	Proti.
19	309	17	10	$2,33 \cdot 10^{-12}$	mediu	15	mediu	3	Pl.	Cern.
20	805	24	22	$9,31 \cdot 10^{-12}$	ridicat	47	ridicat	4	Pl.	Cern.
21	383	16	16	$1,91 \cdot 10^{-11}$	ridicat	23	mediu	3	Hol.	Proti.
22	353	40	41	$1,17 \cdot 10^{-11}$	ridicat	104	ridicat	4	Pl.	Cern.
23	675	29	18	$2,83 \cdot 10^{-12}$	mediu	22	mediu	4	Pl.	Cern.
24	1221	36	109	$4,80 \cdot 10^{-11}$	ridicat	146	ridicat	4	Pl.	Cern.

The χ^2 test confirmed that there was no statistically significant dependence between residential radon concentration and soil radon concentration, radon potential and radon index (p > 0,05).

Table 10. Statistical correlations determined for measured parameters; **correlation is significant at 0,01 level; *correlation is significant at 0,05 level.

Pearson Correlation	CRn_annual	M.G. CRn	M.G. Potential Rn	R.P. Kemski	R.P. Neznal	R.I. Neznal	M.G. perm.	Clasa perm.	GEO.	PEDO.
CRn_annual	X	-0,018	0,317	0,105	0,269	0,187	0,420*	0,143	-0,118	-0,245
M.G. CRn	-0,018	X	0,796**	0,765**	0,758**	0,727**	-0,374	-0,332	0,697**	-0,154
M.G. Potențial Rn	0.317	0,796**	X	0,698**	0,881**	0,818**	0,238	0,137	0,464*	-0,011
R.P. Kemski	0,105	0,765**	0,698**	X	0,862**	0,870**	-0,123	-0,317	0,749**	-0,073
R.P. Neznal	0,269	0,758**	0,881**	0,862**	X	0,891**	0,137	-0,027	0,567**	0,075
R.I. Neznal	0,187	0,727**	0,818**	0,870**	0,891**	X	0,143	0,016	0,653**	-0,084
M.G. perm.	0,420*	-0,374	0,238	-0,123	0,137	0,143	X	0,829**	-0,420*	0,375
Clasa perm.	0,143	-0,332	0,137	-0,317	-0,027	0.016	0,829**	X	-0,494*	0,389
GEOLOGY	-0,118	0,697**	0,464*	0,749**	0,567**	0,653**	-0,420*	-0,494*	X	-0,401
PEDOLOGY	-0,245	-0,154	-0,011	-0,073	0,075	-0,084	0,345	0,389	-0,401	X

5.4. Discussions

Statistical tests showed that, for both residential and soil measurements, the greatest impact on measured values is due to the variable GEOLOGY. Moreover, for the Neznal radon potential and index, as well as for the Kemski geogenic radon potential, only the variable GEOLOGY has a statistically significant impact. For permeability, a higher impact on the values is had by the PEDOLOGY variable, but this is natural in the context that it is the soil that influences the permeability values. The statistically significant impact for the interaction between GEOLOGY and PEDOLOGY for both residential and measured soil gas radon concentrations may be related to the fact that the soil reflects the mineralogical and petrographic characteristics of the parent rocks, hence their radioactivity levels.

There is also a pattern of distribution of values across geological ages and soil classes, but this is normal in that soils will reflect the mineralogical and petrographic characteristics of the parent rocks, hence the level of radioactivity.

Therefore, we can state that, at least for the municipality of Cluj-Napoca, the geological factor seems to control more the geogenic radon concentrations, implicitly the radon potential. Although the same is observed at first sight for residential measurements - in the sense that statistically significant differences were observed for the variables GEOLOGY and PEDOLOGY in terms of radon concentration - we observe that there is no correlation between residential radon concentration and soil radon concentration in the diagnostic phase. With this

test the already known results for the 5 urban settlements in the SMART-RAD-EN project were also verified at local level, i.e. that indoor radon variation does not depend only on soil radon variation. The large discrepancy between residential and measured soil values can also be put in the first instance down to radon potential, as it is known that permeability plays an extremely important role in risk classification for foundation soils (Neznal and Neznal, 2005). However, no correlation was observed between measured indoor values and radon potential, either expressed by the Kemski or Neznal method, in this respect either. Furthermore, if we analyse Table 9, we observe that in the cases of residences 7, 8, 9 and 13, although the Neznal radon potential recorded a low index (including the Kemski geogenic radon potential was classified as class 1), indoor radon concentration values above the reference level of 300 Bq/m^3 were recorded. Most of the other indices were medium (14- 58,3 %) and high (8- 33,3 %).

It is worth noting that, in terms of pedology, in the case of residential measurements where values above 300 Bq/m^3 were recorded, the enclosures overlapped the soils with the best measured permeability (Chenisols and Protisols). Moreover, in the case of measurements on geological tracts, all the soil formations and soil types traversed by radon measurements showed mainly medium and high Neznal radon indices. The same is observed for the Kemski radon potential, where most of the classes are 3 and 4 (meaning above medium-high radon potential), both for geological ages and soil classes. In theory, this means that all these formations and soil types are likely to give indoor radon concentration values above 300 Bq/m^3. Of the total residential measurements, although the same geological epochs and soil classes were covered as for the soil measurements, the values exceeding 300 Bq/m^3 are mostly attributed to the Pleistocene (22, 4 % of the total residential measurements attributed to this period) and the Holocene (12, 4 % of all residential measurements attributed to this period) followed by Oligocene-Miocene (20 % of all residential measurements attributed to this period) and Miocene (1,5 % of all residential measurements attributed to this period). From a pedological point of view, the Protisols have the most overruns (16,5 % of all residential measurements attributed to this soil class) followed by the Chenisols (13,6 % of all residential measurements attributed to this soil class) and the Hydrisols (13 % of all residential measurements attributed to this soil class). In other words, the ratios between radon index, i.e. radon potential (Neznal and Kemski) and exceedances in residential were kept only for Pleistocene and Holocene Chenisols and Protisols. As for the Miocene, which had the third highest frequency in residential measurements, accounting for 23,5 % of the total measurements, and which held 14,3 % of the total high radon indexes and 40,9 % of the total

average indexes, it showed only one exceedance above 300 Bq/m^3, which is 1,5 % of the total residential measurements attributed to this period. Considering all these aspects reported so far, we can state that both the Neznal radon index and potential, as well as the Kemski radon potential and the radon concentration in soil gas do not fully explain the residential radon concentrations and its indoor variation, even at local level, where the measurements were supplemented, on geological trajectories. Thus, they can only provide a rough picture of the geogenic risk for indoor radon.

However, a pattern of distribution of values for radon in soil and residential gas is represented by the Pleistocene, which has preserved the proportions in terms of recorded concentration maxima, means and medians. For residential radon, the Pleistocene showed the highest maxima (1221 Bq/m^3), arithmetic means (192,9 Bq/m^3) and medians (132 Bq/m^3), far from the values attributed to the other geological epochs. For soil radon the Pleistocene also showed the highest maximum (77,7 kBq/m^3) and median (35,8 kBq/m^3) and the second highest arithmetic mean (35,2 kBq/m^3) after the Oligocene-Miocene arithmetic mean (38,9 kBq/m^3) - which showed the second highest maximum (73,8 kBq/m^3) and median (35,2 kBq/m^3). It should be kept in mind, however, that the Oligocene-Miocene accounted for only 5,6 % of all soil measurements and 3,7 % of all residential measurements, giving 5,9 % of all exceedances above the 300 Bq/m^3 limit.

Another distribution pattern is related to the interaction between geological eras and soil classes - Pleistocene vs. Chernisols and Holocene vs. Protisols. However, although soils can explain radon potential through the permeability that influences these values, they cannot directly explain measured radon concentrations in soil. To find an explanation for the measured values, one must look strictly from a geological point of view.

The highest peaks of radon concentration values measured in soil gas are attributed to the Pleistocene, followed in descending order by the Oligocene-Miocene, Miocene, Oligocene, Holocene and Eocene. This order may represent, to some extent, the radioactive potential that the formations attributed to each geological epoch possess.

For the Pleistocene, the values measured in soil gas can be correlated with the source area of the sediments from which the middle and upper terrace deposits of the Somes Mic are made. This includes magmatic rocks, known to have a significant radioactive potential, belonging to the granitic massif of Muntele Mare.

The first author to highlight the relatively high radioactive potential of some waters in Cluj-Napoca, in relation to the source area of quaternary deposits, was Atanasiu (1927, 1931) who, after systematic measurements in the drinking water network of the municipality and other extensive research in the mountain area, concluded that the measured values were a reflection of the radioactive element content in the mineral matrix of the aquifers (large fragments of eruptive rocks, especially granite, which he observed in samples from the digging of wells in Florești). He links the radioactivity measured in the waters to the granitic massif of Maguri-Răcătău and shows that these high values are not only local but common to all the lower terraces and the Someș plain along the valley. Moreover, they observe an increase of the radioactivity value in the waters with the proximity of the granitic massif.

The same trend of increasing radioactivity in the groundwater of the Someşului Mic catchment is also highlighted by the research of Cosma and Baciu (2002) who also show that the measured radon concentration values are related to the presence of endogenous rock fragments with high radioactive content in the alluvium, whose source area is linked to the granitic massif of Măguri-Răcătău. For radon in soil, the same authors report high concentrations, ranging from 18 to 122,2 kBq/m^3, but these values are much more unevenly distributed as one moves upstream.

Moldovan et al. (2013) identify an average radon concentration value of 68.4 Bq/l for groundwater at Măguri-Răcătau, four times higher than the average value obtained for Transylvania, and attribute this to the presence of granite at the surface, which may favour radon accumulation in soil and water.

An unusual fact is that the same source area is also representative for the Holocene deposits of the Someș Mic plain, but these showed lower values than the Pleistocene in terms of soil radon concentration. Also, in the soil gas measurements performed, no increase in radon concentration was observed upstream, the values being unevenly distributed throughout the area.

This may be due to the different evolution of the river in the two geological epochs, as a consequence of large-scale climatic variations influencing river activity oscillations. The transition from glacial (predominantly coarse) to interglacial (predominantly fine) periods and vice versa may trigger an intensification of erosion and aggradation processes, which majorly alter the topography of the watercourse. An indirect manifestation is attributed to the time required for vegetation to react to climate change, which can result in a dramatic change in the

ratio of runoff to available solid flow. This is compounded by the presence of permafrost or seasonal ground frost which may in turn affect the distribution of runoff within the river system (Feier, 2010 and references therein).

Several studies have shown that rivers develop mainly braided patterns during glaciation due to large amounts of coarse-grained sediment and amplified runoff, while in milder periods they show a meandering pattern due to well-developed vegetation, more balanced runoff, and thus limited sediment loading (Nador et al., 2007 and references therein).

Morphological and sedimentary observations of river deposits in central and northwestern Europe have revealed that terraces formed in response to climatic fluctuations generated by Milankovitch cycles (Nador et al, 2003; Brigland and Westway, 2008). At the end of the Pliocene - which recorded a climatic optimum - there is an abrupt degradation and the onset of glacial-interglacial cyclicity that retains the same frequency until the middle Pleistocene, when there is a shift from 41.000-year to 100.000-year Milankovich climate cycles (Head and Gibbard, 2015). Throughout this interval, 100 global climate oscillations have been recorded with amplitudes much larger than those recorded for the Holocene (Feier, 2010, sensu Kukla and Cilek, 1996). After this interval, glacial-interglacial cycles had a stronger impact on runoff, which favoured a shift from extensive river networks (where the width of the river beds was much larger than today and the process of aggradation predominated) to fixed river networks (characterized by a pronounced vertical incision and detachment from the old terraces) (Feier, 2010).

Bridgland and Westaway (2008) show that for most rivers in Europe, although there are a few exceptions, terrace formation occurred at a rate of 1:1 per 100.000-year Milankovitch climate cycle, particularly in the Middle and Upper Pleistocene.

The last major climatic event occurred in the Holocene and is characterised by a sudden rise in temperature, which led to the melting of mountain glaciers and a change in vegetation. This combination of events also led to decreases in the amounts of liquid and solid surface flows in the catchments, and thus to a reduction in the size of the alluvial beds (Feier, 2010).

Pendea et al. (2009), analysing an Upper Pleistocene depositional sequence from Floresti, identify four morphoclimatic stages, the last of which is associated with extreme environmental conditions most likely due to the maximum manifestations of the last Glacial. Pollen studies indicated that, in the last morpho-climatic stage, tree vegetation was completely

removed from the entire region and replaced by grassy vegetation. Under these climatic conditions sedimentation occurred in a high energy system, including wind.

Moreover, Feier (2010) determines the petrographic composition of the fluvial gravels in the bed of the Someș Mic river bed, of Holocene age, and indicates that the main weight in the composition of these deposits is given by the metamorphic material, coming from the crystallophilic formations of the "Seriei de Arada" and Seriei de Someș (crystalline schists and quartzites), a matter that can be explained by the fact that the area of origin of these materials represents most of the drainage area of the upper basin. Magmatic rocks (granite, pegmatite, andesite) have a much smaller participation in the structure of the alluvial material, but this may be a direct consequence of the fact that their source area occupies a much smaller area. However, as it was natural, magmatic rocks have a higher contribution in the area of the river crossing from the mountainous to the depressional zone, but from the granulometric point of view, large-sized clasts in the 64-32 mm granulometric class are missing in the section between Gilău and Dej where the tests were carried out. This is in contradiction with the observations made by Atanasiu (1927), who reports the presence of granite in the alluvial deposits of the lower Florești terrace, in the form of large-sized clasts.

Therefore, in the period attributed to the Last Glacial, both erosion and sediment supply were several orders of magnitude higher than in the Holocene period, which can be translated by a much higher supply of magmatic rocks in the sediments of the lower and upper terraces of the Someș Mic of Pleistocene age, which may be an explanation for the differences recorded for the Pleistocene and Holocene.

It is generally accepted that the radon gas concentration values in the soil reflect the geochemistry of the parent rocks and that geology can explain these values (Gundersen et al., 1988; Gundersen and Schumann, 1996; Kemski et al., 1996; Etiope and Martinelli, 2002; Kemski et al., 2004, 2005; Adepelumi et al., 2005), an aspect that we have also highlighted in the present study.

The need to prevent the harmful effects of radon has led many countries, including Romania, to address this issue from the perspective of defining areas with radon risk potential. The most widely used method at European level was to define risk areas based on indoor radon concentrations, which led to the development of the European radon atlas (Tollefsen et al., 2014). This approach was from the beginning of a purely estimative character, the recommendations being that the (indoor) radon map should not be used as a substitute for

indoor measurements. Furthermore, Bossew (2015) points out that radon data from residential measurements are not sufficient for accurately mapping radon risk and considers that a soil radon potential approach would be more appropriate.

Another attempt has been to relate geology to residential radon, as geology is known to be the most important controlling factor on the distribution of radioactive elements in the substrate, but this approach has also proved insufficient (Appleton and Miles, 2010; Tondeur et al., 2014; De Novellis et al., 2014). Appleton and Miles (2010) show that only 25 % of the total variation in indoor radon concentration in England and Wales can be explained by geology, and Tondeur et al. (2014) indicate that only 15,4 to 17,7 % of the indoor radon variation in the Walloon region of Belgium can be attributed to the geological factor.

Nevertheless, the most appreciated method at present, at international level, is to address the radon risk level as radon potential by itself or in relation to other factors such as geology, house architecture, environmental or anthropogenic factors, etc. (Neznal et al., 2004; Kemski et al., 2005; Ielsch et al., 2010; Pasztor et al., 2016; Yarmoshenko et al., 2016; Ciotoli et al., 2017; Giustini et al., 2019). Although this method provides an improved resolution of the indoor risk potential compared to the previously presented methods, its effectiveness is intensely debated in the circles, especially in terms of a radon risk prediction map.

Friedmann et al. (2017) show in a comprehensive study, which considers correlations between residential radon and soil radon concentration, permeability, soil radium content as well as ambient equivalent dose rate, that all these variables, even when considered together, cannot provide a viable radon risk classification for a given geological region.

All the data and results of the present study underline that none of the variables considered in this scientific approach (soil radon concentration, permeability, radon potential and index, geology, pedology) treated separately or combined with another variable, can only provide an approximate view of the radon risk in a given area and should not be used as a surrogate for indoor measurements.

Chapter 6: Conclusions

The background study, from which the first radon map in soil and water for Romania resulted, showed that, out of the total of 2564 soil measurements with values ranging from 0,2 to 179 kBq/m^3, the arithmetic mean of radon concentration in soil is 29,3 kBq/m^3 and the geometric mean is 24,5 kBq/m^3. In contrast, out of the total 2452 measurements in water, the

arithmetic mean of radon concentration in water was only 9,8 Bq/l, which means that it does not show a significant contribution to indoor radon concentration, unlike the values in soil which can be an explanation for radon measured in dwellings.

Furthermore, some geological patterns were observed in this study with respect to the distribution of measured values. It was observed for radon in soil that high values are characteristic of the metamorphic zones of the Carpathian Units, thus being explained by the chemical composition of the constituent rocks. High values in water were measured in Quaternary deposits in the Western Plain, which was attributed to the source area represented by the western face of the Apuseni Mountains. The highest radon concentrations in water, up to 100 Bq/l, were measured in the mesometamorphic and granitic areas of the Apuseni Mountains.

The first measurements of residential radon in Cluj-Napoca in the first part of the SMART-RAD-EN research project showed that 17,5 % of the investigated residences show values above the reference level. A geological pattern has been observed from this stage of the research that places the highest concentrations in the Quaternary (Holocene and Pleistocene), with the possibility that they are related to the source area of the deposits (the Apuseni granite massif).

As for the study that focused on identifying indoor radon pathways, it indicated, for all participating houses (in all 5 cities), the soil under and around the foundation as the main source of indoor radon. However, no statistically significant correlation was observed between residential and exhaled radon concentration, radon concentration in cracks, radon concentration in soil, radon index and radon potential. This means that radon variation in soil did not directly influence indoor radon variation, and the radon index did not provide sufficient clues to residential radon levels and thus is not recommended to be used as a surrogate for indoor measurements. Moreover, correlations of indoor radon levels and building elements have been identified, leading to the conclusion that, in addition to geology, factors related to such building features and the way houses are used play an important role in indoor radon accumulation and variation.

A tendency was observed for thermally insulated houses to have higher indoor radon concentrations than uninsulated houses, caused by poor natural ventilation. It was also observed that the lack of concrete screed may lead to an increase in the radon exhalation rate.

In Romania, radon concentration values inside buildings (dwellings and public buildings) range from a few tens of Bq/m^3 to several thousands, with the average for the country (at the level of measurements made up to 2017) at 133 Bq/m^3. But this value may not be representative, as indoor radon concentration measurements have covered only one third of the country's area.

Regarding the Cluj-Napoca case study, a pattern of distribution of values according to geological ages and soil types was observed, which is attributed to the fact that soils reflect the mineralogical and petrographic characteristics of the parent rocks.

All the data analysed at this stage indicated that geology has a greater impact than pedology on both radon concentration values measured in the interior or in the soil as well as on Kemski and Neznal radon potentials, including the Neznal radon index. A higher impact is only on permeability values. In the case of residential measurements where values above 300 Bq/m^3 were recorded, residences overlapped the soils with the best measured permeability (Chernisols and Protisols). Thus, the pedology, through its direct influence on permeability, may secondarily influence the values of radon concentrations measured in the soil gas and, through a correspondence relationship, the indoor ones. Although pedology can explain radon potential through the prism of permeability, it could not directly explain radon concentrations measured in soil.

Geologically, measured radon concentration values in soil gas attributed to the Quaternary (Pleistocene and Holocene) can be correlated with the source area of the sediments from which these deposits are made, although significant differences between measured soil radon concentration values have been reported for the Pleistocene and Holocene. These differences can be explained by the different evolution of the Little Someș in the two geological epochs, as a consequence of large-scale climatic variations that influenced oscillations of fluvial activity.

At the level of the municipality of Cluj-Napoca, the measurements carried out by the SMART-RAD-EN project indicate that the annual average values of indoor radon concentration range from a minimum of 10 Bq/m^3 to a maximum of 1221 Bq/m^3 with an arithmetic and geometric mean of 148 and 102 Bq/m^3, respectively, and a median of 91 Bq/m^3. Thus, the mean indoor radon concentration value resulting from both measurement campaigns is higher than the arithmetic mean calculated after the first campaign (139 Bq/m^3), while being

much higher than the mean indoor concentration value of 98 Bq/m^3 reported for Europe, and much closer to the values measured by the Czech Republic and Estonia (140 - 160 Bq/m^3).

The highest indoor radon concentration peaks are attributed to the Pleistocene and Holocene, followed in descending order by the Oligocene-Miocene, Miocene, Eocene and Oligocene.

On the other hand, as regards soil measurements on geological trails, the arithmetic mean of radon concentration values was 25,8 kBq/m^3 and the geometric mean 22,7 kBq/m^3. Minimum values of 4,3 kBq/m^3 and maximum values of 77,7 kBq/m^3 were recorded.

The highest maximum radon concentration values measured in soil gas are attributed to the Pleistocene, followed in descending order by the Oligocene-Miocene, Miocene, Oligocene, Holocene and Eocene. This order may represent a hierarchy of the radioactive potential that the formations attributed to each geological epoch possess, at least in relation to the municipality of Cluj-Napoca.

Geology explains the radon values measured in soil gas, but can only partially explain the radon values measured in the soil gas.

None of the variables considered in this scientific approach can provide satisfactory predictability in terms of indoor radon risk. However, it is worth mentioning that all geological formations showed radon potential values that could theoretically pose problems in terms of indoor radon risk. Moreover, the Pleistocene situation should be treated with utmost interest at the level of Cluj-Napoca municipality.

At present, individual measurement with passive detectors remains the most accurate method to identify and determine indoor radon levels and risk.

On the other hand, radon measurements, whether indoors, in soil or in water, are intended to encourage best practice policies. The study of radon brings together issues from a wide range of fields such as public health, occupational health, environmental protection, green energy, construction, engineering, etc.

Radon risk maps can pose various interpretation problems when used by the general public. The real target audience, however, is the authorities, who have at their disposal an indicator of the need to accelerate public policies aimed at health risk awareness campaigns, building prevention and remediation guidelines, targeted funding allocations and last but not

least alignment with international policies. Moreover, as with the cancer risk from smoking, the health effect of radon needs systematic, consistent and complex studies.

The present study is the first scientific approach of its kind in Romania and can be seen as a useful link in the complex chain of radon investigations. This thesis addresses for the first time, at national level, the complex study of indoor radon and geogenic radon in relation to geology and pedology, and draws the first conclusions regarding radon risk prediction. At the same time, new data in the field of radon research have been provided in terms of indoor radon sources and pathways. The data from the measurements also provide a broader view of the radon risk in specific areas of the country and also at local level in the case of the study focused on the municipality of Cluj-Napoca.

The prediction of indoor radon risk, as well as geogenic risk, remains an open issue for future studies. Although the statistical methods we used in this study are widely used, they may have some limitations. Indoor radon concentration is influenced by a number of variables that are difficult to quantify and much more difficult to analyse, taken together, by classical statistical methods. In the future we want to address this issue with AI and machine learning software that can allow simultaneous analysis of quantitative and qualitative data that can lead, in theory, to indoor radon risk prediction with high accuracy.

A number of other variables will be considered in future studies, such as the content of other radioactive elements in soils and geological formations (Uranium, Thorium, Radium, Potassium, etc.), as well as architectural and construction details of houses. The latter should be grouped and classified according to common variables, and included in a publicly accessible database. We also aim to identify other new variables that will contribute to a better understanding of radon generation, transport, emanation and accumulation phenomena.

References

Adepelumi, A.A., Ajayi, T.R., Ojo, O., 2005. Radon soil-gas as a geological mapping tool: case study from basement complex Nigeria. Environmental Geology, 48: 762-770.

Ahmad, R., Wilson, C.J.L., 1981. Uranium and boron distributions related to metamorphic microstructure-evidence for metamorphic fluid activity. Contributions in Mineralogy and Petrology, 76: 24-32.

Al-Khateeb, H.M., Aljarrah, K.M., Alzoubi, F.Y., Alqadi, M.K., Ahmad, A.A., 2017. The correllation between indoor and in soil radon concentrations in a desert climate. Radiation Physics and Chemistry, 130: 142-147.

Appleton, D.J., Miles, J.C.H., 2010. A statistical evaluation of the geogenic controls on indoor radon concentrations and radon risk. Journal of Environmental Radioactivity, 101(10): 799-803.

Atanasiu, G., 1927. Radioactivitatea apei potabile din Cluj și valoarea ei medicală. Clujul Medical, 5: 3-30.

Atanasiu, G., 1931. Radioactivite des sources d'eau de Roumanie. III. Anuarul Institutului Geologic al României, 16: 935-943.

Baciu, C., Filipescu, S., 2002. Structura geologică. In: Cristea, V., Baciu, C., Gafta, D. (eds.). Municipiul Cluj-Napoca și zona periurbană. Studii Ambientale, 25-36 pp.

Balintoni, I., 1997. Geotectonica terenurilor metamorfice din România. Editura Carpatica, Cluj Napoca, 176 pp.

Basic safety standards for protection against the dangers arising from expo-sure to ionising radiation. Council Directive 2013/59/Euratom Jan 17, 2014. 73 pp.

Beaubien, S.E., Ciotoli, G., Lombardi, S., 2003. Carbon dioxide and radon gas hazard in the Alban Hills area (Central Italy). Journal of Volcanology and Geothermal Research, 123(1-2): 63-80.

Bossew, P., 2015. Mapping the Geogenic Radon Potential and Estimation of Radon Prone Areas in Germany. Radiation Emergency Medicine, 4: 13-20.

Bridgland, D. R., Westaway, R., 2008. Preservation patterns of Late Cenozoic fluvial deposits and their implications: results from IGCP 449. Quaternary International, 189: 5-38.

Burchfiel, B.C., 1976. Geology of Romania. Geological Society of America, Special Paper, 158: 82 pp.

Burghele, B., Ţenter, A., Cucoş, A., Dicu, T., Moldovan, M., Papp, B., Szacsvai, K., Neda, T., Suciu, L., Lupulescu, A., Maloş, C., Florică, Ş., Baciu, C., Sainz, C., 2019. The FIRST large-scale mapping of radon concentration in soil gas and water in Romania. Science of the Total Environment, 669: 887-892.

Cinelli, G., De Cort, M., Tollefsen, T., 2019. European Atlas of Natural Radiation, Publication Office of the European Union, Luxembourg, 190 pp.

Ciotoli, G., Voltaggio, M., Tuccimei, P., Soligo, M., Pasculi, A., Beaubien, S.E., 2017. Geographically weighted regression and geostatistical techniques to construct the geogenic radon potential map

of the Lazio region: A methodological proposal for the European Atlas of Natural Radiation. Journal of Environmental Radioactivity, 166: 355-375.

Cosma, C., Jurcuţ, T., 1996. Radonul şi mediul înconjurător. Editura Dacia, Cluj-Napoca, 208 pp.

Cosma, C., Baciu, C., 2002. Dinamica radonului. In: Cristea, V., Baciu, C., Gafta, D. (eds). Municipiul Cluj- Napoca şi zona periurbană. Studii Ambientale: 79-88.

Cosma, C., Moldovan, M, Dicu, Kovacs, T, 2008. Radon in water from Transylvania (Romania). Radiation Measurements, 4(8): 1423-1428.

Cosma, C., Dicu T., Dinu, A., Begy, R., 2009. Radonul şi cancerul pulmonar, seria Radioactivitatea mediului II. Ed. Quantum-EFES, 169 pp.

Cosma, C., Cucoş-Dinu, A., Papp, B., Begy, R., Sainz, C., 2013. Soil and building material as main sources of indoor radon in Băiţa-Ştei radon prone area (Romania). Journal of Environmental Radioactivity, 116: 174-179.

Cross, F.B., 1998. Facts and values in risk assessment. Reliability Engineering and System Safety, 59(1): 27-40.

Cucoş, A., Papp, B., Dicu, T., Moldovan, M., Burghel,e B.D., Moraru, I.T., Ţenter, A., Cosma, C., 2017. Residential, soil and water radon surveys in north-western part of Romania. Journal of Environmental Radioactivity, 166: 412-416.

Cucoş (Dinu), A., Cosma, C., Dicu, T., Begy, R., Moldovan, M., Papp, B., Niţă, D., Burghele, B., Sainz, C., 2012. Thorough investigations on indoor radon in Băiţa radon-prone area (Romania). Science of the Total Environment (1); 431:78-83.

Cumberland, S.A., Douglas, G., Grice, K., Moreau, J.W., 2016. Uranium mobility in organic matter-rich sediments: A review of geological and geochemical processes. Earth-Science Reviews, 159: 160-185.

Darby, S., Hill, D., Auvinen, A., Barros-Dios, J.M., Baysson, H., Bochicchio, F., Deo, H., Falk, R., Forastiere, F., Hakama, M., Heid, I., Kreienbrock, L., Kreuzer, M., Lagarde, F., Mäkeläinen, I., Muirhead, C., Oberaigner, W., Pershagen, G., Ruano-Ravina, A., Ruosteenoja, E., SchaffrathRosario, A., Tirmarche, M., Tomásek, L., Whitley, E., Wichmann, H.-E., Doll, R., 2005. Radon in homes and risk of lung cancer: collaborative analysis of individual data from 13 European case-control studies. British Medical Journal, 330(7485): 223.

Darby, S., Hill, D., Deo, H., Auvinen, A., Barros-Dios, J.M., Baysson, H., Bochicchio, F., Falk, R., Farachi, S., Figueiras, A., Hakama, M., Heid, I., Hunter, N., Kreienbrock, L., Kreuzer, M., Lagarde, F., Mäkeläinen, I., Muirhead, C., Oberaigner, W., Pershagen, G., Ruosteenoja, E.,

Schaffrath Rosario, A., Tirmarche, M., Tomásek, L., Whitley, E., Wichmann, H.-E., Doll, R., 2006. Residential radon and lung cancer - detailed results of a collaborative analysis of individual data on 7148 persons with lung cancer and 14208 persons without lung cancer from 13 epidemiologic studies in Europe. Scandinavian Journal of Work, Environment & Health, 32: 1-84.

De Novellis, S., Pasculli, A., Palermi, S., 2014. Innovative modeling methodology for mapping of radon potential based on local relationships between indoor radon measurements and environmental geology factors. WIT Transactions on Information and Communication Technologies, 47(9): 109-119.

Dinu, A.L., 2009. Corelații între radonul din locuințe și incidența cancerului pulmonar în zona minieră Ștei-Băița. Teză de doctorat, Universitatea Babeș-Bolyai, Cluj-Napoca, 166 pp.

Euratom, 2014. Council Directive 2013/59/Euratom of 5 December 2013 laying down basic safety standards for protection against the dangers arising from exposure to ionising radiation, and repealing Directives 89/618/Euratom, 90/641/Euratom, 96/29/Euratom, 97/43/Euratom a. Official Journal of the European Union L13(1).

Etiope, G., Martinelli, G., 2002. Migration of carrier and trace gases in the geosphere: an overview. Physics of the Earth and Planetary Interiors, 129(3-4): 185-204.

Fărcaș, C., 2011. Studiul formațiunilor continentale Eocen terminale și Oligocen timpurii din NV-ul Depresiunii Transilvaniei - biostratigrafie și reconstituiri paleoambientale, pe baza asociațiilor de vertebrate continentale. Rezumatul Tezei de doctorat, Universitatea Babeș-Bolyai din Cluj Napoca, 50 pp.

Feier, I., 2010. Reconstituirea evoluției geomorfologice a văii Someșului Mic în Eocen. Teză de doctorat, Facultatea de Geografie-Geologie, Universitatea Al. I. Cuza, Iași, 276 pp.

Filipescu, S., 2011. Cenozoic lithostratigraphic units in Transylvania. In: Bucur, I., Săsăran, E. (eds.). Calcareous algae from Romanian Carpathians. Field trip Guidebook. Presa Universitară Clujeană, 37-48.

Florea, N., Asvadurov, H., 1994. Harta solurilor Republicii Socialiste România. Foaia 10 Cluj, L-34-XII, 1:200.000. Institutul de Cercetări pentru Pedologie și Agrochimie, București

Florică, Ș., Dicu, T., Burghele, B.D., Moldovan, M., Szacsvai, K., Țenter, A., Papp, B., Beldean, S., Istrate, A., Catalina, T., Tunyagi, A., Horju-Deac, C., Răchișan, A., Sferle, T., Dobrei, G., Sainz, C., Cucoș, A., 2017. Indoor radon related with the geology in Romanian urban aglomerations (Cluj-Napoca). Studia UBB Ambientum, 62(2): 29-36.

Florică, Ș., Burghele, B.D., Bican-Brișan, N., Begy, R., Codrea, V., Cucoș, A., Catalina, T., Dicu, T., Dobrei, G., Istrate, A., Lupulescu, A., Moldovan, M., Niță D., Papp, B., Pap, I., Szacsvai, K., Țenter, A., Sferle, T., Sainz, C., 2020. The path from geology to indoor radon, Environmental Geochemistry and Health, 42: 2655–2665.

Foerster, E., Beck, T., Buchroder, H., Doring, J., Schmidt, V., 2016. Intruments to measure radon-222 activity concentration or exposure to radon-222-Intercomparison 2015, Salzgitter, 48 pp.

Foerster, E., Friedrich, F., Dubslaff, M., Schneider, F., Doring, J., 2019. Messgeräte zur Bestimmung der Radon-222-Aktivitätskonzentration oder der Radon-222-Exposition Vergleichsprüfung 2018/ Instruments to Measure Radon-222 Activity Concentration or Exposure to Radon-222 – Interlaboratory comparison 2018, Salzgitter, 50 pp.

Friedmann, H., Baumgartner, A., Bernreiter, M., Graser, J., Gruber, V., Kabrt, F., Kaineder, H., Maringer, F.J., Ringer, W., Seidel, C., Wurm, G., 2017. Indoor radon, Geogenic radon surrogates and geology – Investigations on their correlation. Journal of Environmental Radioactivity, 166: 382-389.

Friedrich, F., Foerster, E., Dubslaff, M., Schneider, F., Feige, S., 2019. Messgeräte zur Bestimmung der Radon-222-Aktivitätskonzentration oder der Radon-222-Exposition Instruments to measure radon-222 activity concentration or exposure to radon-222-Interlaboratory comparison and proficiency testing 2019, Salzgitter, 48 pp.

Giustini, F., Ciotoli, G., Rinaldini, A., Ruggiero, L., Voltaggio, M., 2019. Mapping the geogenic radon potential and radon risk by using Empirical Baesyan Kriging regression: A case study from a volcanic area of central Italy. Science of the Total Environment, 661: 449-464.

Gundersen, L.C.S., Reimer, G.M., Wiggs, C.R., Rice, C.A., 1988. Radon potential of rocks and soils in Montgomery County, Maryland. U.S. Geological Survey Miscellaneous Field Studies Map, Series Number: 2043.

Gundersen, L.C.S., Schumann, R.R., 1996. Mapping the radon potential of the United States: Examples from the Appalachians. Environment International, 22(1): 829-837.

Hanomolo, I.M., Hanomolo, A., 1962. Geologia și petrografia regiunii Someș-Muntele Rece-Măguri-Mănăstireni-Căpuș. Dări de Seamă ale Comitetului Geologic, 67: 97-113.

Head, M. J., Gibbard, P.L., 2015. Early-Middle Pleistocene transitions: an overview and recommendation for the defining boundary. Geological Society, London, Special Publication, 247: 1-18.

Hosu, A., 1999. Arhitectura sedimentaţiei depozitelor Eocene din nord-vestul Depresiunii Transilvaniei. Presa Universitară Clujeană, Cluj-Napoca, 224 pp.

IARC, 1988 International Agency for Research on Cancer (IARC) Lyon. Man-made mineral fibres and radon. IARC Monographs on the Evaluation of Carcinogenic Risk to Humans, 309 pp.

ICRP (International Commission on Radiological Protection), 2007. Publication 103, The 2007 recommendations of the International Commission on Radiological Protection.

Ielsch, G., Cushing, M.E., Combes, P., Cuney, M., 2010. Mapping of the geogenic radon potential in France to improve radon risk management: methodology and first application to region Bourgogne. Journal of Environmental Radioactivity, 101: 813-820.

Keith, S., Doyle, J.R., Harper, C., Mumatz, M., Tarrago, O., Wohlers, W.D., Diamond, G.L., Citra, M, Barber, L.E., 2012. Toxicological Profile for Radon. Atlanta (GA): Agency for Toxic Substances and Disease Registry (US), Atlanta, Georgia, 378 pp.

Kemski, J., Klingel, R., Siehl, A., 1996. Clasification and mapping of radon-affected areas in Germany. Environment International, 22(1): 789-798.

Kemski, J., Siehl, A., Stegemann, R., Valdivia-Manchego, M., 2004. Mapping the geogenic radon potential in Germany. The Science of the Total environment, 272: 217-230.

Kemski, J., Klingel, R., Siehl, A., Stegemann, R., 2005. Radon transfer from ground to houses and prediction of indoor radon in Germany based on geological information. Radioactivity in the environment, 7: 820-832.

Klepper, M.R., Wyant, D.G., 1957. Contribution to the geology of uranium. Geological Survey Bulletin 1046-F. United States Government Printing Office, Washington, 148 pp.

Krézsek, C., Bally, A.W., 2006. The Transylvanian Basin (Romania) and its Relation to the Carpathian Fold and Thrust Belt: Insights in Gravitational Salt Tectonics. Marine and Petroleum Geology, 23(4): 405-442.

Kukla, G.J. Cilek V., 1996. Plio-Pleistocene megacycles: record of climate and tectonics. Palaeogeography. Palaeoclimatology. Palaeoecology, 120: 171-194.

Law nr. 301/2015 establishing the requirements for protection of human health as regards radioactive substances in drinking water (published: 2015-12-07).

Lazăr, C., Întorsureanu, I., 1982. Contribuții la cunoașterea zăcământului de fier de la Mașca-Băișoara – Munții Apuseni. Dări de Seamă ale Ședințelor, Institul de Geologie și Geofizică 66(2): 45-69.

Leung, S.S.Y., Nikezic, D., Leung, J.K.C., Yu, K.N., 2007. Sensitivity of LR 115 SSNTD in a diffusion chamber. Nuclear Instruments and Methods in Physics Research, 263: 306-310.

Manual tehnic sistem RM-2. Soil Radon Monitoring System RM-2, User Manual, Radon V.O.S., producer: Dr. Froňka, Nuclear Technology, Czech Republic.

Mészáros, N., Clichici, O., 1976. Pe poteci cu banuței de piatră. Ghid geologic al zonei Cluj. Editura Sport-Turism, București, 166 pp.

M.O. 752/3.978/136/2018, Ordinul ministrului sănătății, al ministrului educației naționale și al președintelui Comisiei Naționale pentru Controlul Activității Nucleare nr. 752/3.978/136/2018 pentru aprobarea Normelor privind cerințele de bază de securitate radiologică. Monitorul Oficial al României, Partea I, Nr. 517 bis/25.VI.2018.

M.O. Partea I, Nr. 655/7.VII.2019, Ordin privind aprobarea Metodologiei pentru determinarea concentrației de radon în aerul din interiorul clădirilor și de la locurile de muncă, 2019.

Moldovan, M., Niță, D.C., Costin, D., Cosma, C., 2013. Radon concentration in ground water from Măguri Răcătău area, Cluj county. Carpathian Journal of Earth and Environmental Sciences, 8(3): 81-86.

Murariu, T., 2005. Geochimia și metalogenia uraniului. Editura Universității Alexandru Ioan Cuza, Iași, 430 pp.

Mureșan, I., 1974. Contributions a l'étude des banatites et des pyroclastites de la bordure du Nord-Est des Montagnes Gilău. Bulletin de Volcanologie 38(4): 1157-1180.

Mureșan, I., 1980. Geologia și petrografia bordurii de nord-est a Munților Gilău. Editura Academiei Republicii Socialiste Româna, 127 pp.

Mutihac, V., 1990. Structura geologică a teritoriului României. Editura Tehnică, București, 418 pp.

Mutihac, V., Ionesi, L., 1974. Geologia României. Editura Tehnică, București, 646 pp.

Nador, A., Lantos, M., Toth-Makk, A., Thamo-Bozso, E., 2003. Milankovitch-scale multi-proxy records from fluvial sediments of the last 2.6 Ma, Pannonian Basin, Hungary. Quaternary Science Reviews, 22: 2157-2175

Nador, A., Thamo-Bozso, E., Magyari, A., Babinszki, E., 2007. Fluvial responses to tectonics and climate change during the Late Weichselian in the eastern part of the Pannonian Basin (Hungary). Sedimentary Geology 202: 174-192

Neznal, M., Neznal, M., Matolín, M., Barnet, I., Mikšová, J., 2004. The new method for assessing the radon risk of building sites. Czech Geological Survey Special Papers, Prague, 7-47.

Neznal. M., Neznal. M., 2005. Permeability as an important parameter for radon risk classification of foundation soils. Annals of Geophysics, 48(1): 175-180.

Papp, B., 2011. Radonul și fluxul de radon din sol. Aplicații în mediu, Geologie și geofizică. Teză de doctorat, Universitatea Babeș-Bolyai, Cluj-Napoca, 146 pp.

Papp, B., Cucoş (Dinu), A., Cosma, C., 2017. A comprehensive study of residential, geogenic and water radon in the North area of Mures county, Romania. Radiation Protection Dosimetry, 179(1): 80-86.

Paraschiv, D., 1979. Romanian Oil and Gas Fields. Institutul de Geologie şi Geofizică, Studii Tehnice şi Economice, Bucharest, A(13): 382 pp.

Pasztor, L., Ssabo, K., Szatmari, G., Laborcsi, A., Horvath, A., 2016. Mapping geogenic radon potential by regression kriging. Science of the Total Environment, 544: 883-891.

Pendea, I.F., Gray, J.T., Ghaleb, B., Tanţău, I., Bădărău, A.S., Nicorici, C., 2009. Episodic build-up of alluvial fan deposits during the Weichselian Pleniglacial in the western Transylvanian Basin, Romania and their paleoenvironmental significance. Quaternary International, 198: 98-112.

Piciu, T., Simihăian, M., Stan, G., 2002. Aspecte pedologice. In: Cristea, V., Baciu, C., Gafta, D. (eds.). Municipiul Cluj-Napoca și zona periurbană. Studii ambientale. Editura Accent, 25-36.

Plch, J., 2008. Manual for Operating LUK 3P Device, M.Eng. SMM, Prague, 29 pp.

Popescu, B., 1984. Litostratigraphy of cyclic continental to marine eocene deposits in NW Transylvania, Romania. Archives des Sciences - Université de Genève, 37(1): 37-73.

Rallakis, D., Michels, R., Brouand, M., Parize, O., Cathelineau, M., 2019. The role of organic matter on uranium precipitation in Zoovch Ovoo, Mongolia. Minerals, 9(5): 310.

Răileanu, G., Saulea, E., 1967. Republica Socialistă România, Harta Geologică. Foaia 10 Cluj, L-34-XII, 1:200.000. Comitetul de Stat al Geologiei, Institutul Geologic, București.

RIM (2018). International comparison measurement of radon in soil gas at radon reference sites Cetyne and Buk in the Czech Republic, 17 September 2018. TECHICAL REPORT.

RIM (2021). International comparison measurement of radon in soil gas at radon reference sites Cetyne and Buk in the Czech Republic, 17 September 2018. TECHICAL REPORT.

Răileanu, G., Saulea, E., 1967. Republica Socialistă România, Harta Geologică. Foaia 10 Cluj, L-34-XII, 1:200.000. Comitetul de Stat al Geologiei, Institutul Geologic, București.

Rusu, A., 1970. Corelarea faciesurilor Oligocenului din regiunea Treznea-Bizușa (NV Bazinului Transilvaniei). Studii și Cercetări Geologie, Geofizică, Geografie. Seria Geologie, 15(2): 513-525.

Săndulescu, M., 1984. Geotectonica României. Editura Tehnică, București, 335 pp.

Săndulescu, M., Visarion, M., 1978. Considérations sur la structure tectonique du soubassement de la Dépression de Transylvanie. Dări de Seamă Institutul de Geologie și Geofizică, 64: 153-173.

Săndulescu, M., Kräutner, H., Borcoș, M., Năstăseanu, S., Patrulius, D., Ștefănescu, M., Ghenea, C., Lupu, M., Savu, H., Bercia, I., Marinescu, F., 1978. Geological map of Romania, 1:1,000,000. Geological Institute of Romania Printing House, Bucharest.

Săndulescu, M., 1988. Chapter 2: Cenozoic Tectonic History of the Carpathians. In: Royden, L.H., Horvath, F. (eds.). The Pannonian Basin: A Study in Basin Evolution. American Association of Petroleum Geologists, Special Volumes, 113: 17-25.

Săsăran, L., Săsăran, E., 2003. Facies analysis of the Late Cretaceous deposits from Corni Quarry (North-Eastern border of Gilău Mountains). Studia UBB Geologia, 48(2): 81-94.

Săsăran, L., 2011. Upper Cretaceous deposits from the North-Eastern edge of Gilău Mountains (Northern Apuseni Mountains). In: Bucur, I., Săsăran, E. (eds.). Calcareous algae from Romanian Carpathians, 33-36.

Stoici, S.D., Tătaru, S., 1988. Uraniul și Thoriul. Editura Tehnică, București, 338 pp.

Ștefan, A., Lazăr, C., Întorsureanu, I., Horvath, A., Gheorghiță, I., Bratosin, I., Șerbănescu, A., Călinescu, E., 1985. Petrological Study of the Banatic Eruptive Rocks in the Eastern Part of the Gilău Mountains. Dări de Seamă ale Insitutului Geologic și Geofizic, 69: 215-247.

Ștefan, A., Lazăr, C., Berbeleac, I., Udubașa, G., 1988. Evolution of banatitic magmatism in the Apuseni Mts. and associated metallogenesis. Dări de Seamă ale Institulului Geologic și Geofizică, 72-73(2): 195-213.

Ștefan, A., Roșu, E., Andar, A., Robu, L., Robu, N., Bratosin, I., Grabari, G., Vajdea, E., 1992. Petrological and geochemical features of banatitic magmatites in northern Apuseni Mountains. Romanian Journal of Petrology, 75: 97-115.

Tollefsen, T., Cinelli, G., Bossew, P., Gruber, V., De Cort, M., 2014. From the European indoor radon map towards an atlas of natural radiation; Radiation Protection Dosimetry, 162: 129-134.

Tondeur, F., Cinelli, G., Dehandschutter, B., 2014. Homogenity of geological units with respect to the radon risk in Wallon region of Belgium. Journal of Environmental Radioactivity, 139: 140-151.

Tunyagi, A., Dicu, T., Cucoș, A., Burghele, B.D., Dobrei, G., Lupulescu, A., Moldovan, M., Niță, D., Papp, B., Pap, I., Szacsvai, K., Țenter, A., Beldean-Galea, M.S., Anton, M., Grecu, Ș., Cioloca, L., Milos, R., Botos, M.L., Chiorean, C.G., Catalina, T., Istrate, M.A., Sainz, C., 2020. An innovative system for monitoring radon and indoor air quality. Romanian Journal of Physics, 65: 1-14.

Ud-Din Khan, S., Nakhabov, A., 2020. Nuclear Reactor Technology development and Utilization. Fuel Cycles, Advanced Reactors, and Hybrid Systems. In Woodhead Publishing Series in Energy, Elsevier, 492 pp.

UNSCEAR (United Nations Scientific Comittee on the Effects of Atomic Radiation), 2008 Report. Sources and effects of ionizing radiation. Vol. 1: Sources, 2008.

Vlaicu-Tâtărâm, N., 1963. Stratigrafia Eocenului din regiunea de la Sud-Vest de Cluj. Editura Academiei Republicii Socialiste România, 204 pp.

WHO (World Health Organisation), 2009. WHO Handbook on Indoor Radon: A Public Health Perspective. Hajo, Z., Ferid, S., (eds.), Geneva, 94 pp.

WHO, 2011. Guidelines for Drinking-water Quality. Fourth edition. World Health Organisation, Geneva, 541 pp.

Yarmoshenko, I., Malinovsky, G., Vasilyev, A., Onischenko, A., Seleznev, A., 2016. Geogenic and anthropogenic impacts on indoor radon in the Techa River region. Science of the Total environment, 571: 1298-1303.

Zhukovsky, M., Onischenko, A., Bastrikov, V., 2010. Radon measurements-discussion of error estimates for selected methods. Applied Radiation and Isotopes, 68: 816-820.